B.R.1600A
Code No.1563
A.P.1093E(2)

Chapter 16

RECEPTION OF RADIO-FREQUENCY PULSES

List of Contents

CHAPTER 16

RECEPTION OF RADIO-FREQUENCY PULSES

INTRODUCTION

1. General

In radar equipments the transmitted RF pulse possesses a more or less rectangular waveform; (Fig. 652). After transmission and reflection from the target the pulse returned to the equipment has approximately the same shape but is very much weaker. The ideal receiver should be capable of receiving the weakest possible reflected pulse without distorting its shape or introducing any noise.

In Chap. 15 it has been shown that unavoidable noise power is generated in any receiver and it is this noise power which ultimately limits the sensitivity and fidelity of pulse reception. A compromise design must be adopted and it is therefore inevitable that careful attention is given to the problem of noise when radar receiver design is under consideration.

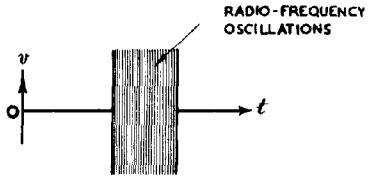

Fig. 652 - Radio-frequency pulse of rectangular waveform.

Clearly the maximum possible sensitivity should be secured in the receiver, anything less than this wasting transmitted power, and it is therefore usual to find that radar receivers have sufficient maximum gain to produce saturation or near-saturation outputs from inherent noise alone.

The distortion of the RF pulse in the receiver is important for two different reasons :-

(i) If the Range difference to two separate targets corresponds to a time interval greater than half the duration of the transmitted pulse, then the target echoes are received separately ; otherwise the two responses partially coincide. The resolving power in distance is therefore limited by the duration of the emitted pulse, and any increase of pulse length due to receiver distortion will reduce this resolving power, i.e. there will be a loss in Range discrimination.

(ii) An attempt is made to keep the leading edge of the reproduced pulse as abrupt as possible, particularly when measurement of this leading edge is used for the determination of Range. Any loss of steepness of this edge due to distortion in the receiver results in a corresponding loss of accuracy of Range measurement.

In a radar equipment, the direct signal from the nearby transmitter produces extremely large voltages in the receiver. These voltages, which may persist for a time considerably longer than the transmitted pulse, usually render the receiver insensitive to signals. This effect is known as Paralysis, and unless it is minimised or overcome the receiver will be incapable of responding adequately to signals from targets at close range.

The receivers in normal use in radar employ the Superheterodyne principle. An arrangement, shown in Fig.653, consists of RF Amplifiers,

a Mixer (Frequency Changer) and Local Oscillator, IF (Intermediate Frequency) Amplifiers, a Detector, and Video Frequency Amplifiers. The radio frequencies in normal use in radar lie in the range 30 Mc/s. to 10,000 Mc/s. It has not yet been found possible to produce useful amplification at frequencies greater than about 700 Mc/s.; hence, in Radar receivers operating at frequencies greater than this, the RF Amplifiers are omitted. Idealised waveforms of the pulse to be expected at different stages of the receiver are shown in Fig. 654.

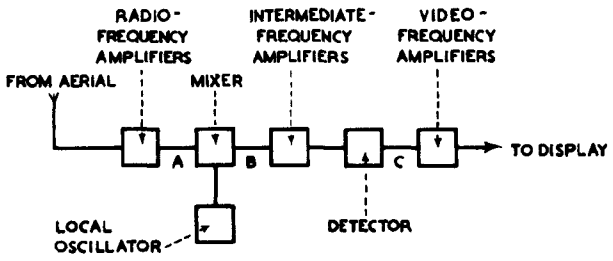

Fig. 653 - Block diagram of superheterodyne receiver.

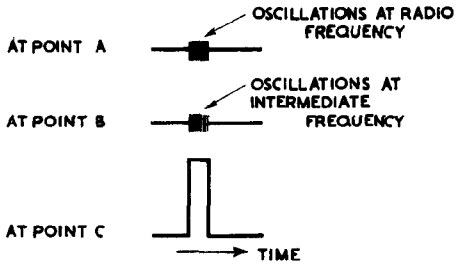

Fig. 654 - Idealised waveforms of pulse at various points of the superheterodyne receiver shown in fig. 653.

2. Fourier Analysis

The signal which is transmitted and received by Radar equipments is ideally a rectangular-shaped RF pulse (Fig. 652) of short duration (1/10 to 10 microseconds). The Bandwidth of the receiver which is required to receive such pulses without undue distortion can be calculated.

Consider the succession of pulses shown in Fig. 655. If these are exactly similar in shape and are repeated at regular intervals of time ($\frac{1}{F}$) they can be analysed as a Fourier spectrum consisting of a number of sinusoidal components of different amplitude, frequency and phase. In the case under consideration, assuming that one pulse is located symmetrically about an axis representing zero time, the components have a cosine variation, i.e., the instantaneous value of each is a maximum at zero time. The Fourier series corresponding to the waveform of Fig. 655 is thus :-

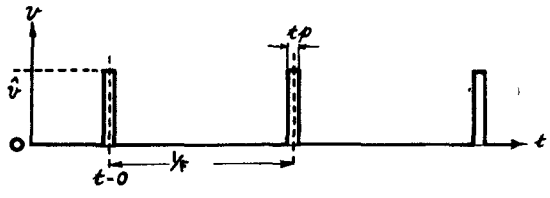

Fig. 655 - Succession of rectangular pulses.

$v = a_o + a_1 \cos \omega t + a_2 \cos 2\omega t + a_3 \cos 3\omega t + \ldots\ldots$to infinity

where $\omega = 2 \pi F.$ ..... (1)

There is thus a steady component of value a_o, a component of amplitude a_1 and of frequency equal to the repetition frequency of the pulses (fundamental component, or first harmonic), together with an infinite number of components which are harmonics of this frequency.

If each pulse is of amplitude $\hat{v}$ and duration t_p, calculation shows that the value of the steady component is $\hat{v} F t_p$, the amplitude a_1 of the fundamental is $\frac{2\hat{v}}{\pi} \sin \pi F t_p$ and the amplitude a_n of the nth harmonic

$$\frac{2\hat{v}}{n\pi} \sin n \pi F t_p .$$

Harmonics of such an order that $n \pi F t_p$ is equal to a multiple of π have zero amplitude. These components have frequencies $\frac{1}{t_p}$, $\frac{2}{t_p}$, $\frac{3}{t_p}$, etc., and their positions on the amplitude spectrum are known respectively as the first, second, third, etc., zeros. A typical amplitude spectrum, for pulses of one volt amplitude, one microsecond duration and of repetition frequency 400 per second is shown, as far as the third zero, in Fig. 656. In theory the spectrum covers an infinite range of frequencies. Since t_p = 1 microsecond the zeros are spaced 1 Mc/s. apart, the individual components being separated by 400 c/s., i.e., by the repetition frequency of the pulses. There are thus 2,500 components between zero frequency and the first zero of the spectrum, so that a large scale is required if the individual components are to be represented, as they should be, by discrete lines.

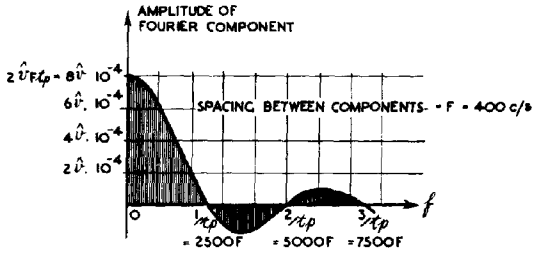

Fig. 656 - Spectrum of recurrent rectangular pulses with a repetition period = 2500 X pulse duration.

It is shown in the Standard Service Manuals (see BR 230 (Admiralty Handbook of Wireless Telegraphy, Vol II) Sec. N para. 15, and AP 1093 Chap. XII para. 14 for a more detailed analysis) that a continuous sinusoidal oscillation of frequency f_o, amplitude modulated at a frequency f_m, behaves as though it were composed of three sinusoidal components of constant amplitude and of frequencies f_o, $f_o + f_m$ and $f_o - f_m$ respectively. This simple example is illustrated in Fig. 657, and the equation of the modulated wave is :-

$$v = (\hat{v}_o + \hat{v}_m \cos \omega_m t) \cos \omega_o t$$

$$= \hat{v}_o \cos \omega_o t + \tfrac{1}{2} \hat{v}_m \cos (\omega_o + \omega_m)t + \tfrac{1}{2} \hat{v}_m \cos (\omega_o - \omega_m)t$$

where $\omega_o = 2 \pi f_o$ and $\omega_m = 2 \pi f_m$. ..... (2)

The three components are known as the carrier, upper sideband and lower sideband respectively. The amplitude spectrum is shown in Fig. 658. It should be noted that the carrier amplitude $\hat{v}_o$ is equal to the average value of the modulated carrier, and the amplitudes of the sidebands are each equal to half the amplitude of the modulating oscillation.

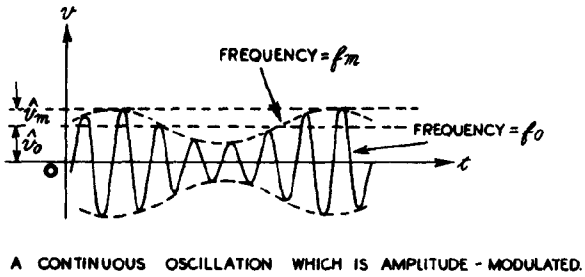

A CONTINUOUS OSCILLATION WHICH IS AMPLITUDE - MODULATED.

Fig. 657 - A continuous oscillation which is amplitude-modulated.

When the modulation envelope is not a pure sine wave it may be analysed into a Fourier series and each harmonic in this series will give rise to its own pair of sidebands. The greater the number of harmonics in the modulating waveform the more numerous are the sidebands and the wider is the spread of the frequency spectrum on each side of the carrier.

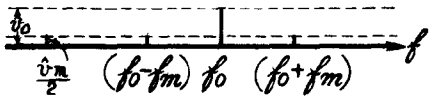

Fig. 658 - Amplitude spectrum of the amplitude-modulated oscillation shown in fig. 657.

It has already been shown that a succession of pulses (Fig. 655) can be considered as consisting of sinusoidal components (Equation (1)). Hence if the successive RF pulses shown in Fig. 659 are exactly similar in shape, are repeated at regular intervals and are Coherent, i.e., they are the result of amplitude modulation of a continuous sinusoidal oscillation, the equation representing these pulses will be :-

$$v = \cos\omega_{ot}\,(a_o + a_1 \cos\omega t + a_2 \cos 2\omega t + a_3 \cos 3\omega t + \ldots\ldots\ldots)$$

where $\omega = 2\pi F$

$$= a_o \cos \omega_o t \ldots\ldots\ldots\ldots\text{(carrier)}$$

$$+ \tfrac{1}{2} a_1 \cos(\omega_o + \omega)t + \tfrac{1}{2} a_1 \cos(\omega_o - \omega)t \quad \text{(first sidebands)}$$

$$+ \tfrac{1}{2} a_2 \cos(\omega_o + 2\omega)t + \tfrac{1}{2} a_2 \cos(\omega_o - 2\omega)t \quad \text{(second sidebands)}$$

$$+ \tfrac{1}{2} a_3 \cos(\omega_o + 3\omega)t + \tfrac{1}{2} a_3 \cos(\omega_o - 3\omega)t \quad \text{(third sidebands)}$$

$$+ \text{etc.} \qquad \ldots\ldots\ldots\ldots\ldots\ldots\ldots\ldots\ldots\ldots (3)$$

The carrier amplitude is therefore $\hat{v}\,Ft_p$ and the sideband amplitudes $\frac{\hat{v}}{\pi} \sin \pi Ft_p$, $\frac{\hat{v}}{2\pi} \sin 2\pi Ft_p$, $\frac{\hat{v}}{3\pi} \sin 3\pi Ft_p$, etc. If the pulse recurrence frequency is 400/sec. and the pulse duration 1 microsecond as before, the amplitude spectrum for $\hat{v} = 1$ volt and $f_o = 500$ Mc/s. is shown in Fig. 660.

The changes which take place in the amplitude spectrum in the transition from the recurrent pulses of Fig. 655 to the recurrent coherent

RF pulses of Fig. 659 may now be seen. The steady component of magnitude $\hat{V}Ft_p$ becomes the carrier component having the same peak amplitude, whilst each of the harmonic components of Fig. 656 splits into a pair of sidebands of half the amplitude and symmetrically disposed with respect to the carrier. Given Fig. 656 it is thus possible to derive Fig. 660 by this simple process.

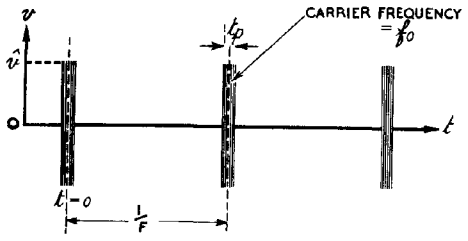

Fig. 659 - Recurrent radio-frequency pulses.

In practice the RF pulses received by radar equipments are not repeated at exactly equal intervals of time, and successive pulses are likely to be slightly different in duration and amplitude. Also such pulses are usually not coherent in the sense described above; i.e., the radio-frequency oscillation starts afresh in each pulse and there is no phase linkage from one pulse to the next. The effect of these variations in duration, amplitude and radio-frequency phase is to "blur" the spectrum so that it no longer consists of discrete frequency components, without, however, altering its general nature.

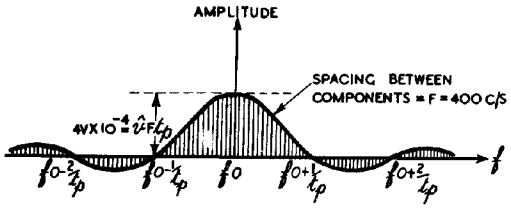

Fig. 660 - Amplitude spectrum of recurrent RF pulses with a repetition period = 2500 × pulse duration.

It has been shown that the periodic train of pulses shown in Fig. 655 consists of sinusoidal components of frequencies F, 2F, 3F, etc. As the repetition frequency is reduced the components thus become correspondingly closer in frequency; at the same time the amplitude of each is reduced. In the limiting case of a single pulse the components become indefinitely close together, thus forming a continuous spectrum, while the amplitudes are vanishingly small. However it may be shown that the relative amplitudes of the components are still given by the envelope of Fig. 656. This argument applies equally well to the RF pulses of Fig. 659 and is the basis of the Fourier Integral treatment of the single RF pulse.

In radar, single RF pulses are not used, the recurrence frequency seldom being less than 400 c/s. However, the amplitude-frequency spectrum is more accurately portrayed as a continuous or "White" spectrum rather than one composed of discrete harmonic components, for the following reasons :-

(i) As already remarked, the pulses are not coherent, there being no phase linkage between successive transmitted pulses.

(ii) The transmitter frequency is liable to vary by an amount sufficient to blur the spectrum completely.

E.G., suppose the recurrence frequency is 1000 c/s. For a centimetre equipment a random frequency-variation of 1000 c/s between successive pulses is not unlikely. Hence the positions of the harmonic components of the spectrum are completely random.

(iii) The pulse width t_p and recurrence frequency F, and therefore the envelope of the amplitude-frequency spectrum, are liable to random variations.

3. Distortion of RF Pulse During Amplification

As described in Chap. 7 Sec. 8, in order to amplify satisfactorily RF pulses of the type shown in Fig. 652 an RF amplifier must exhibit amplitude-frequency and phase-frequency characteristics of the types shown in Fig. 341. These characteristics are drawn in an idealised form in Fig. 661., and a comparison with Fig. 660 shows that with such characteristics the higher order sidebands are inevitably removed in the amplifier. The wider the pass band the more accurately is the pulse envelope reproduced; but at the same time the noise is increased, and it is therefore necessary to adopt a compromise, the exact nature of which depends on the requirements of the particular radar application.

In the first instance we may calculate the response of an idealised band-pass amplifier, possessing characteristics such as those shown in Fig. 661, to a succession of coherent RF pulses. The response of such an amplifier to one of these pulses is illustrated in Fig. 662.

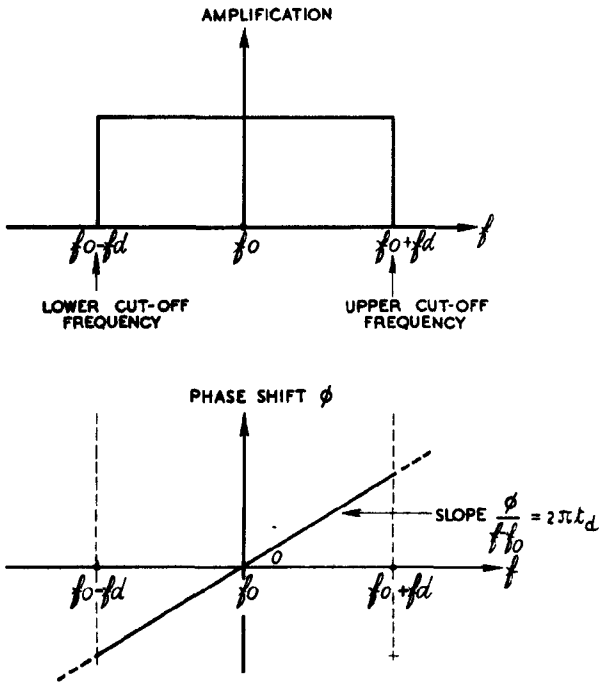

Fig. 661 - Amplitude and Phase-Shift characteristics of idealised band-pass amplifier.

The input pulse is shown at (a), while (b) and (c) show the shape of the output pulse for bandwidths of $\frac{2}{t_p}$ and $\frac{8}{t_p}$ respectively; (b) therefore corresponds to the inclusion of all the sidebands of Fig. 660 as far as the first zero on each side of the carrier; in (c) the sidebands between the fourth zeros are included. The leading edge of the reproduced pulse is curved and the convention of Fig. 663 is adopted for estimating the delay time and time of rise. If the input voltage v_i were sinusoidal, of frequency f_o, the output would have amplitude $\hat{v}_o = |m| \hat{v}_i$. This amplitude is used as

a reference level when the input voltage is in the form of a RF pulse, also of amplitude $\hat{v}_i$, and the point X is taken when the pulse amplitude has risen to $\frac{1}{2}\ |m|\ \hat{v}_i$. The tangent at this point intersects the zero and $|m|\ \hat{v}_i$ levels at P and Q respectively. The time difference between these two points is taken to be the time of rise tr of the reproduced pulse, and the delay time t_d is taken as the time difference between X and the leading edge of the input pulse.

With these definitions it may be shown that :-

(1) $t_d = \frac{1}{2\pi} \times$ (slope of phase characteristic of Fig.661).

(2) $t_r = \frac{1}{B}$, where B is the bandwidth, $2f_d$ (Fig.661).

(3) the oscillations at the top of the pulse of Fig. 662 (c) have a frequency of $\frac{B}{2}$ c/s.

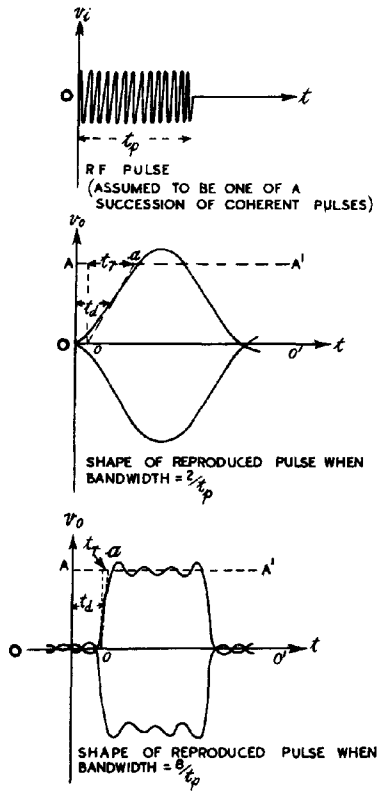

Fig. 662 - Distortion of a RF pulse by an idealised band-pass amplifier.

The response of the idealised amplifier discussed above is in the main close to that of a practical amplifier, i.e., the delay, time of rise and frequency of oscillations are much the same in the two cases. However, in practice, each successive pulse may be treated as distinct from those preceding it, since the pulses are not coherent, and if this is done it is obvious that no oscillations due to this pulse can occur before t = 0, i.e., there can be no output before the input is applied.

Investigation into the transmission properties of practical amplifiers shows that, if the amplification characteristic displays sharp cut-offs, the phase-shift characteristic is excessively non-linear at the extremities of the pass band. As a consequence, pronounced oscillations (overshoots) occur during and after the time interval of the reproduced RF pulse; (Fig. 664(a)). In radar systems, the overshoots, in so far as they constitute deviations from a true rectangular shape, should be

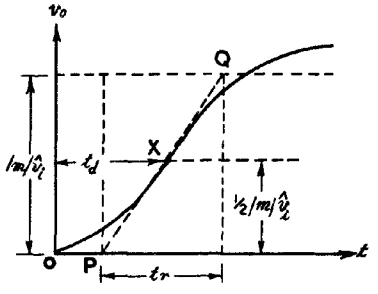

Fig. 663 - Delay-time and time of rise of reproduced pulse.

avoided. This is particularly important in systems in which the target is indicated by a change in the brilliance of the trace on the CRT. The effect of such overshoots on the display can be minimised by the processes of Pulse Limitation and Clamping (see Chaps. 9 and 12). If the amplification characteristic of the amplifier displays gradual cut-offs, the phase-shift characteristic is not excessively non-linear, and the overshoots are comparatively small in amplitude; Fig. 664(b). In general, however, for a given pass band, a more gradual cut-off in the amplification characteristic means a slower rise in the leading edge of the reproduced pulse.

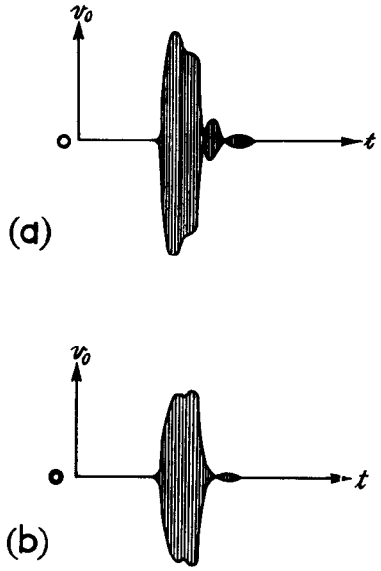

Fig. 664 - Reproduction of a rectangular RF pulse by a RF amplifier with (a) sharp cut-off and (b) gradual cut-off.

4. The Effect of Noise

All radar receivers possess inherent noise voltages which are in general of random amplitude and phase throughout all frequencies. Since the noise energy present in a given circuit is in most cases proportional to the bandwidth over which the circuit is responsive, the RMS value of the noise voltage is proportional to the square root of the bandwidth. The phase characteristic does not enter into the calculation of the average noise power since the phases of the noise voltages are purely random and therefore their effect, averaged out over an interval of time, is the same regardless of the phase-shift characteristic of the circuit. The noise voltages are amplified with the signal and produce on an A-type display the typical picture already described in Chap. 15 and illustrated in Fig. 642 In general, if the amplitude of a received pulse, applied to the deflecting plates of a CRT, is less than that of the noise voltages, it cannot be seen through the noise. This limits the maximum Range at which the equipment can detect signals. To increase the maximum Range, and to make the indication of signals more reliable at all ranges, it is clearly desirable to reduce as far as possible the noise voltages relative to the signal voltages.

Suppose that a RF pulse of duration t_p is applied to a circuit, the amplification of which may be kept constant as its bandwidth is varied. Starting with a narrow bandwidth the noise voltages will be small, but the rate of rise of the leading edge of the reproduced pulse will be so slow that the pulse will not have sufficient time to build up to its full amplitude (Fig. 665). As the bandwidth is increased the amplitudes of both pulse and noise increase also but the ratio of pulse to noise increases at first, passes through a maximum and then decreases; (Fig. 666). The optimum condition, $B = B_o$, depends to some extent on the type of display used, the recurrence frequency, etc.; for optimum detection of small signals on an A-display, B_o is usually chosen between $\frac{1}{t_p}$ and $\frac{2}{t_p}$.

If it is desirable in a radar equipment to make accurate range measurements or to discriminate between closely neighbouring echoes,

faithful reproduction of the pulse shape is of greater importance than optimum signal/noise ratio, and the bandwidth used in such equipments may be as great as $\frac{10}{t_p}$. Naturally this accuracy of pulse reproduction is obtained only by a sacrifice of maximum Range. A useful working compromise between fidelity of pulse shape and accuracy of Range measurement is to choose a bandwidth of about twice the optimum, i.e., an equipment transmitting a 1 microsecond pulse will have a receiver bandwidth of about 2-4 Mc/s.

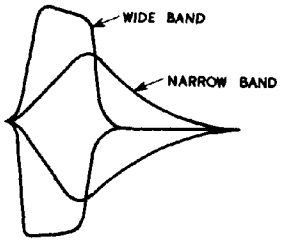

ENVELOPE OF REPRODUCED PULSE SHOWING EFFECT OF REDUCTION OF BAND WIDTH AT CONSTANT GAIN.

Fig. 665 - Envelope of reproduced pulse showing effect of reduction of bandwidth at constant gain.

The choice of pulse duration will again depend on the purpose of the equipment. For any given pulse length t_p the bandwidth for optimum signal/noise ratio is proportional to $\frac{1}{t_p}$ so that a relatively long pulse implies a narrow bandwidth with a corresponding reduction in noise. The use of a long pulse of the same peak power will therefore lead to an improvement in signal/noise ratio and an extension of maximum Range. In general, early warning equipments have fairly long pulses and narrow receiver bandwidths but poor discrimination, whereas for good Range discrimination the pulse is short, the receiver bandwidth wide and the Range limited.

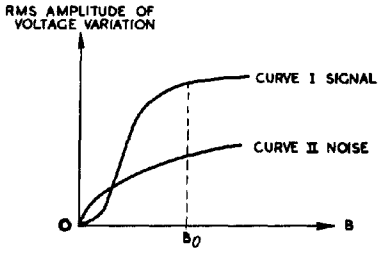

Fig. 666 - Variation of signal and noise output voltages with bandwidth of circuit.

5. The Superheterodyne Principle

It has been stated that radar receivers normally employ the superheterodyne principle. This is used in order to obtain the necessary high gain with stability. Further, on centimetre wavelengths no useful signal frequency amplification is possible, so that a change of frequency is essential. At the same time, selectivity is not a problem as it is in communications working, and the receiver bandwidth is determined solely by pulse fidelity and signal/noise considerations and not by the necessity of avoiding interference from transmissions on adjacent channels. Similarly, the choice of the intermediate frequency is not dictated by second-channel interference problems. This is not to say that radar receivers are immune from interference, but such interference is of a specialised character and is not removed by merely restricting receiver bandwidth.

The effect of the frequency-changer is to shift the pulse spectrum of Fig. 660 so that it is no longer centred about the signal frequency but about the intermediate frequency, the relative amplitudes and positions of the sidebands remaining unchanged. The considerations discussed above in connection with the bandwidth of circuits designed to pass RF pulses apply equally well to circuits used for amplification at the intermediate frequency. In fact it is in the IF amplifier that the necessary bandwidth is obtained; the signal frequency circuits, owing to

the higher working frequency are usually much more flatly tuned. This corresponds with normal communications practice.

The necessity for amplifying a short RF pulse and the consequent wide bandwidth needed restricts the choice of the intermediate frequency. For a given bandwidth and tuning capacitance the gain of a RF amplifier is independent of the mid-band frequency so that stability considerations suggest the use of a low value of IF: on the other hand there must be a sufficiently large number of IF cycles to "fill in" the pulse envelope. At least 20 cycles are needed for this purpose, so that for the accurate reproduction of 1 microsecond pulses an IF of at least 20 Mc/s. would be needed. Longer pulses could be dealt with at correspondingly lower frequencies, e.g. a 5-microsecond pulse could be handled by an IF amplifier working on 4 Mc/s. Where accurate reproduction of the pulse shape is not required a smaller number of IF cycles can be tolerated, as few as 5 cycles per pulse being satisfactory in some cases.

A further advantage of not using a high IF is that certain sources of noise are thereby avoided; (see Chap. 15 Sec. 10).

The output from the IF amplifier is applied to the detector, the output of which should ideally consist of a rectified pulse having the same shape as the envelope of the IF pulse. Since all sideband components up to $\frac{B}{2}$ on each side of the carrier have been retained in the IF amplifier the output from the detector may be analysed into a frequency spectrum extending from zero up to an upper limit of $\frac{B}{2}$ c/s. For distortionless detection these components should be maintained with correct relative amplitudes and correct relative phase. However, the detector must always incorporate some filter device to remove the residual intermediate frequency components, together with harmonics which are inevitably produced in the detection process. The higher the IF chosen the easier it is to filter out the unwanted IF components and their harmonics without introducing amplitude or phase changes in the frequency range 0 - $\frac{B}{2}$ c/s. The choice of at least 20 IF cycles per pulse enables this to be done without difficulty.

Similarly the video-frequency stages following the detector should reproduce the output of the latter without distortion; i.e. the video stages should have uniform amplitude/frequency and linear phase/frequency characteristics up to at least $\frac{B}{2}$ c/s.

6. Typical 200 Mc/s Radar Receiver

The following are the details of a typical radar equipment:-

(1) Signal frequency : 200 Mc/s.
(2) Intermediate frequency : 45 Mc/s.
(3) Pulse length : 3 microseconds. (There are thus 135 IF cycles per pulse.)
(4) IF bandwidth B = 3 Mc/s. (With this value of $\frac{10}{t_p}$, accurate reproduction of the pulse is obtained, the time of rise of the leading edge being 0·33 microseconds.)
(5) Video amplifiers : Amplitude/frequency characteristic flat up to 2 Mc/s. (Since only sidebands up to 1·5 Mc/s. on each side of the carrier are passed by the IF amplifier the video amplifier need only handle frequencies up to 1·5 Mc/s., but the extension of the video frequency range beyond that actually required improves the amplifier characteristics. In particular, the phase characteristic tends to become excessively non-linear at the upper

end of the range; with 2 Mc/s. upper frequency limit this non-linear portion is outside the band of frequencies handled by the amplifier.)

INFLUENCE OF NOISE FACTORS ON RF AMPLIFICATION

7. General

In Sec. 4 some of the more general problems relating to noise in receivers are discussed, showing how unavoidable noise sets an upper limit to the maximum Range obtainable with a radar equipment. In this section we consider in greater detail how noise affects the design of RF amplifiers and of valves used in such amplifiers. The term Radio Frequency will be taken to include both Signal Frequency and Intermediate Frequency. The effects of noise in Frequency Changers will be dealt with in Secs. 24-28.

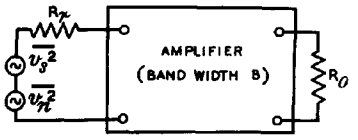

Fig. 667 - Block diagram of ideal RF amplifier.

8. The Ideal RF Amplifier

In an ideal RF amplifier all the valves and circuits would be completely free of noise and the signal/noise ratio at the output of such an amplifier would depend on the aerial alone. Consider the block diagram of Fig. 667, the amplifier being considered to be free from noise and to have ideal amplitude/frequency and phase/frequency characteristics over an adequate band-width B. The output impedance of the aerial, its radiation resistance R_r (see Chap. 17 Sec. 11), and the input and output impedances of the amplifier, R_ℓ and R_o, are assumed to be pure resistances over the bandwidth B. The input circuit is shown in Fig. 668. During the pulse the signal power present in R_o will be $|m|^2$ times the signal power present in R_ℓ where $|m|$ is the amplification. Similarly the noise power in R_o will be $|m|^2$ times the noise power in R_ℓ associated with the bandwidth B since only those frequency components of noise lying within the pass band can affect the output.

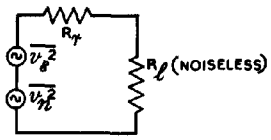

Fig. 668 - Input circuit of ideal RF amplifier.

Let $\overline{v_s^2}$ be the mean square signal voltage in the aerial during the pulse. The signal power P_s is then given by

$$P_s = \frac{R_\ell}{(R_r + R_\ell)^2} \cdot \overline{v_s^2} \quad \ldots\ldots\ldots\ldots\ldots\ldots\ldots\ldots (1).$$

Similarly, the noise power P_n, is given by

$$P_n = \frac{R_\ell}{(R_r + R_\ell)^2} \cdot \overline{v_n^2} \quad \ldots\ldots\ldots\ldots\ldots\ldots\ldots\ldots (2).$$

where $\overline{v_n^2}$ is the mean square noise voltage in R_r associated with the bandwidth B;

i.e., $$\overline{v_n^2} = 4kTBR_r = KR_r, \quad \ldots\ldots\ldots\ldots\ldots\ldots\ldots\ldots (3),$$

where K = 4kTB.

The ratio of noise/signal power at the input is thus

$$P_n/P_s = KR_r/\overline{v_s^2} \quad \ldots\ldots\ldots\ldots\ldots\ldots\ldots\ldots\ldots\ldots\ldots\ldots\ldots\ldots (4),$$

which is also the noise/signal power in R_ℓ. This ratio (4) is independent of R_ℓ so that the signal/noise ratio in an ideal amplifier is independent of the aerial matching conditions.

9. The Practical RF Amplifier: Noise Factor

In an actual amplifier R_ℓ is noisy and there is also noise in the valves and other components, the net result being that the ratio of noise/signal power in the output is higher for a real amplifier than for an ideal one. This deterioration is expressed by the Noise Factor F which is defined as :-

$$F = \frac{\text{Noise/signal power in output of real amplifier}}{\text{Noise/signal power in output of ideal amplifier}} \quad \ldots\ldots (5),$$

F, being in effect a power ratio, may be expressed either as a pure number or in decibels; e.g. F = 4 or F = 6 db.

In order that the noise factor of an amplifier may be as low as possible careful consideration must be given to the design of the first stage. Since the signal and noise outputs of this stage in particular are amplified together by all succeeding stages it is clearly desirable that the noise/signal ratio at the first grid should be as low as possible.

Consider the circuit of Fig. 669 in which an aerial of resistance R_r is shown inductively coupled to the first tuned circuit of the amplifier by a perfect transformer, of turns ratio 1:n. In practice the transformer will not be perfect, the circuit will not necessarily consist of lumped inductance and capacitance and some reactance may be present in the aerial. These differences will not, however, invalidate the argument which follows; they will merely complicate the mathematics without affecting the general conclusions.

10. Input Circuit Coupling with Noiseless First Valve

In communications practice where noise is not the limiting factor the turns ratio n is usually chosen to give maximum signal at the grid. This condition is obtained when the aerial resistance is matched to the dynamic resistance R_d of the tuned circuit, i.e. when

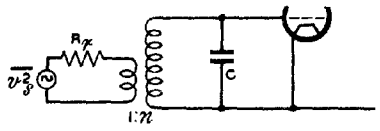

Fig. 669 - Input circuit of first stage of amplifier.

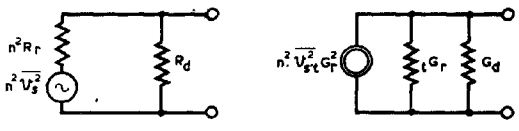

Fig. 670 - Equivalent signal circuits of fig. 669.

$$n^2 R_r = R_d \quad \ldots\ldots\ldots\ldots\ldots\ldots\ldots\ldots\ldots\ldots\ldots\ldots\ldots\ldots (6)$$

The equivalent circuits of Fig. 669 are shown in Fig. 670, the current circuit (b) being the easier to work with when noise calculations are required, since the use of conductances instead of resistances leads to a simplification of the algebra. $t^{G}r$ is the Transferred Aerial Conductance and is equal to $\frac{1}{n^2 R_r} = \frac{G_r}{n^2}$. From Fig. 670 (b) the mean square signal voltage at the grid is

$$\overline{{}_s v_i^2} = n^2 . \overline{v_s^2} . {}_t G_r^2 . \frac{1}{({}_t G_r + G_d)^2} ,$$

$$= \frac{G_r \, . \, {}_t G_r}{({}_t G_r + G_d)^2} . \overline{v_s^2} \qquad \ldots\ldots\ldots\ldots\ldots\ldots\ldots\ldots (7)$$

and this is a maximum when ${}_t G_r = G_d$. This is the same result as that given by equation (6), in terms of conductances instead of resistances.

It is now possible to see how the coupling between aerial and tuned circuit needs to be modified when noise is present. Considering the noise in the tuned circuit alone, i.e. assuming for the moment that the valve is noiseless, the mean square noise voltage $\overline{{}_n v_i^2}$ at the grid within the band-width B is found from the equivalent circuit of Fig. 671. It is

$$\overline{{}_n v_i^2} = \frac{K ({}_t G_r + G_d)}{({}_t G_r + G_d)^2} \qquad \ldots\ldots\ldots\ldots\ldots\ldots\ldots\ldots (8)$$

Dividing (8) by (7), we obtain

$$\frac{\overline{{}_n v_i^2}}{\overline{{}_s v_i^2}} = \frac{K ({}_t G_r + G_d)}{{}_t G_r \cdot G_r \cdot \overline{v_s^2}} \qquad \ldots\ldots\ldots\ldots\ldots\ldots\ldots\ldots (9)$$

but for the ideal amplifier

$$\frac{\overline{{}_n v_i^2}}{\overline{{}_s v_i^2}} = \frac{K R_r}{\overline{v_s^2}} = \frac{K}{G_r \, \overline{v_s^2}} \qquad \ldots\ldots\ldots\ldots\ldots\ldots\ldots\ldots (10)$$

from (4).

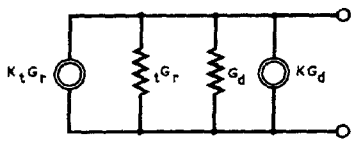

Fig. 671 - Equivalent noise circuit of fig. 669 (valve assumed noiseless).

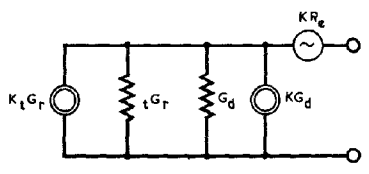

Fig. 672 - Equivalent noise circuit of fig. 669 with noisy valve.

By definition, the noise factor F is the quotient of (10) and (9) so that

$$F = \frac{{}_t G_r + G_d}{{}_t G_r} = 1 + \frac{G_d}{{}_t G_r} \qquad \ldots\ldots\ldots\ldots\ldots\ldots\ldots\ldots (11)$$

It follows from (11) that there is no optimum coupling from the noise point of view, the value of F decreasing asymptotically to unity as $t^{G}r$ increases. For the matched condition, in which maximum signal is obtained at the grid, the noise factor F is equal to 2. This condition should now be avoided and the transferred aerial conductance made as large as possible. The signal naturally suffers but the all-important ratio of signal-to-noise is improved.

In RF amplifiers used in radar receivers it is customary to connect resistors in parallel with the tuned circuits to obtain the necessary band-width. In the case of the first tuned circuit this should not be done, for such a resistor would increase the dynamic conductance G_d of the tuned circuit and thus increase the noise factor; (equation (11)). The damping imposed by the transferred aerial conductance is usually sufficient to give an adequate band-width.

11. Input Circuit Coupling with Noisy First Valve

As an introduction to the effects of valve noise it will now be assumed that shot and partition noise are present in the first stage. The circuit of Fig. 671 is then modified by the inclusion of the valve noise generator between the circuit and the grid; (Fig. 672). Since this generator is a purely fictitious one, i.e. there is no resistance of value R_e anywhere in the circuit, it cannot be transformed into an equivalent current generator and similarly there is no advantage in expressing the equivalent noise resistance as a conductance. The mixture of current and voltage generators and conductances and resistances of Fig. 672 not only simplifies the algebra but also emphasizes the distinction between resistances which represent energy losses and those which are merely convenient mathematical devices for representing noise magnitudes.

It follows from Fig. 671 and 672 that the mean square noise voltage at the grid in the latter case is

$$\overline{{}_{n}v_{1}^{2}} = \frac{K\,(t^{G}r + G_d)}{(t^{G}r + G_d)^2} + K\,R_e \quad \ldots\ldots\ldots\ldots\ldots \quad (12)$$

The signal voltage is unchanged by the introduction of the additional noise generator so that the mean square signal voltage is

$$\overline{{}_{s}v_{1}^{2}} = \frac{G_r\ t^{G}r}{(t^{G}r + G_d)^2} \cdot \overline{v_s^2} \quad \ldots\ldots\ldots\ldots\ldots\ldots \quad (13)$$

as before.

Dividing (12) by (13) and then by (10) we obtain the noise factor :-

$$F = 1 + \frac{G_d}{t^{G}r} + \frac{(t^{G}r + G_d)^2}{t^{G}r} \cdot R_e \quad \ldots\ldots\ldots\ldots\ldots \quad (14)$$

It is now found that there is an optimum value of G_r, giving a minimum noise factor. If (14) is differentiated and the derivative equated to zero the optimum value of $t^{G}r$ is found to be :-

$$t^{G}r\ (\text{opt}) = G_d\sqrt{\frac{1+x}{x}}\ ; \quad \text{where } x = G_d\,R_e \quad \ldots\ldots\ldots \quad (15)$$

and the minimum noise factor is :-

$$F = 1 + 2x + 2\sqrt{x + x^2} \quad \ldots\ldots\ldots\ldots\ldots\ldots\ldots \quad (16)$$

It follows from (15) that the best value of $t^{G}r$ is always greater than that required for matching ($t^{G}r = G_d$) since $\frac{1+x}{x}$ is always greater than unity.

The noisier the valve, the greater the value of x and the smaller the optimum t^Gr. In the extreme case where the valve noise over-rides the circuit noise, (15) reduces to $t^Gr = G_d$, which expresses the obvious conclusion that when valve noise predominates the best signal/noise ratio is obtained when the signal at the grid is a maximum.

With a given value of equivalent noise resistance R_e the variation of noise factor and band-width with t^Gr is shown in Fig. 673. Curve F(I) shows the change of noise factor with t^Gr when valve noise is absent, while curve F(II) shows the corresponding case in which R_e= 1400 ohms, a value which is appropriate to a CV1091 valve. It will be noted that a transferred aerial conductance which is slightly greater than the optimum is needed in the latter case to give a band-width of 4 Mc/s, the deterioration in noise factor due to this being only 0·15 db. When other sources of damping which have so far been neglected are taken into account the band-width is more than adequate when the noise factor is a minimum.

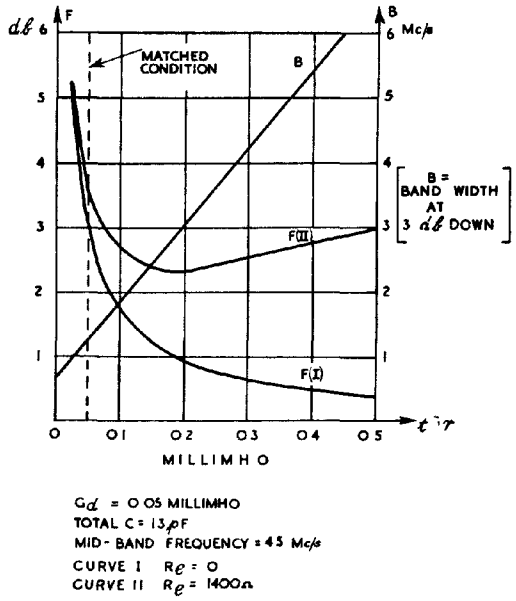

Fig. 673 - Noise factor and band-width of circuit of fig. 672.

We may use the curves of Fig. 673 to compare the noise factors under matched and optimum conditions. For the matched aerial F = 3·62 db, whereas the minimum noise factor is 2·36 db. This improvement of 1.26 db is equivalent to a 34% increase in transmitter power.

12. Effects of Transit Time and Cathode Lead Inductance

It has been shown in Chap. 7 Sec. 25 that at high frequencies, when the time of transit of an electron through the valve becomes an appreciable fraction of the input cycle, energy is absorbed from the input circuit. Alternatively it may be said that the valve has a finite input conductance due to transit time. This transit time input conductance G_t is effectively in parallelwith the tuned circuit, casu ng both a loss of signal and an increase in bandwidth. As stated in Chap. 15 Sec. 10, the mean square noise current at the grid within the frequency band B due to transit time only (Induced Grid Noise) may usually be taken as

$$\overline{g i_n^2} = 4kTB.4\cdot8G_t \qquad \ldots\ldots\ldots\ldots\ldots\ldots\ldots\ldots\ldots\ldots(17)$$

so that the transit time input conductance is about five times as noisy as an equal physical conductance at the same temperature. The effect of transit time in the valve on the circuit of Fig. 669 is to add the noisy

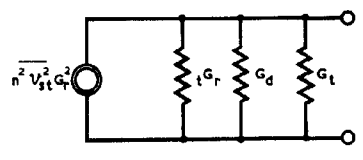

Fig. 674 - Equivalent signal circuit of fig. 670(b) with addition of transit time conductance.

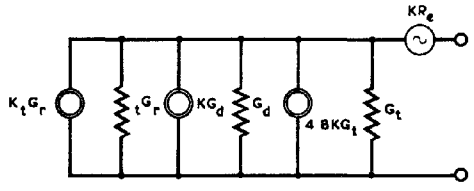

Fig. 675 - Equivalent noise circuit of fig. 672 with addition of transit time (induced grid) noise.

transit time conductance in parallel with the tuned circuit, giving the equivalent signal and noise circuits of Figs. 674 and 675 respectively.

When transit time noise and shot noise are combined as in Fig. 675 it is not at once clear that the linear addition of mean square voltages is valid, since such addition is strictly true only for random independent events such as noise contributions from two distinct sources. Now transit time and shot noise are not independent, both being produced by the same electron stream; however, a more detailed study of the frequency spectrum of the noise shows that for any given component of this spectrum the transit time and shot noise are effectively in phase quadrature, at least for the small transit angles normally encountered in practice. The mean square voltages may thus be added linearly to give the total effect, just as if they were produced by independent sources.

In any valve operated with its cathode nominally earthed (grounded-cathode circuit) it is essential to have a certain length of lead between cathode and earth, if only to prevent undue conduction of heat from the hot cathode to the seal through the glass. This cathode lead possesses inductance which affects the input impedance of the stage. Referring to Fig. 676, if L_K is the inductance of the cathode lead and C_{gk} the grid-cathode capacitance, then it has been shown in Chap. 7 Sec. 25 that the input conductance is :-

$$G_K = \omega^2 . L_K . C_{gk} . G_m \quad \ldots\ldots\ldots\ldots\ldots\ldots (18).$$

This is the conductance which is in parallel with the input circuit at the dotted line PQ of Fig. 676. The input circuit to the left of PQ may be replaced by a current generator in parallel with the output conductance G_o so that the equivalent signal circuit is that of Fig. 677.

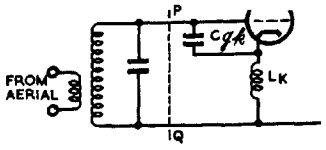

Fig. 676 - Input circuit of grounded-cathode stage showing cathode lead inductance.

It is now necessary to consider what noise generator (if any) should be associated with conductance G_K. A distinction must be made between the shot noise and partition noise which have hitherto been lumped together in a single noise generator, since the shot noise currents are present in the cathode lead whereas the partition noise currents are not. (See Chap. 15 Sec. 15). If the frequency spectrum of the shot noise is considered, any one component of this spectrum will produce a voltage across L_K (Fig. 676), and will thus be injected into the series circuit formed by L_K, C_{gk} and the input circuit. A consideration of the amplitude of the resultant current shows that the voltage developed across C_{gk} produces negative feedback of the noise and that the magnitude of this feedback is correct if the shot noise generator is placed as in Fig. 678 and the input conductance G_K is noiseless. The noise present in the circuit to the left of PQ in Fig. 676 is represented by the current generator $\overline{i_n^2}$ and R_p, the partition noise generator, is placed in its usual position, since such noise is not subject to feedback.

Suppose that for the moment partition noise is neglected; then the mean square signal voltage at the grid (Fig. 677) is:

$$\overline{s v^2} = \overline{i_s^2} \cdot \frac{1}{(G_o + G_K)^2} \quad \ldots\ldots\ldots\ldots\ldots\ldots (19),$$

while the mean square noise voltage (Fig. 678) is:

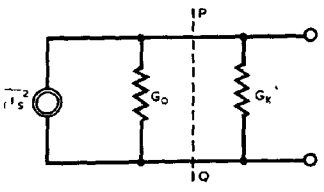

Fig. 677 - Equivalent signal circuit of fig. 676.

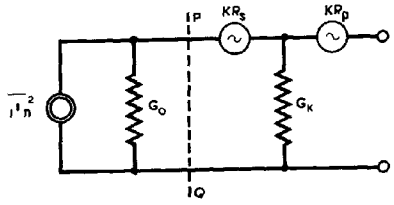

Fig. 678 - Equivalent noise circuit of fig. 676.

$$\overline{n_v^2} = \overline{i_n^2} \cdot \frac{1}{(G_o + G_K)^2} + \frac{KR_s G_o^2}{(G_o + G_K)^2} \quad \ldots\ldots\ldots(20).$$

The noise/signal ratio is therefore:

$$\frac{\overline{n_v^2}}{\overline{s_v^2}} = \frac{\overline{i_n^2}}{\overline{i_s^2}} + \frac{KR_s G_o^2}{\overline{i_s^2}} \quad \ldots\ldots\ldots\ldots\ldots\ldots\ldots\ldots(21),$$

which is independent of G_K and is therefore the same as if G_K were absent. Since the current generator of Fig. 678 includes the effect of transit time it follows that the inverse feedback due to cathode lead inductance affects all sources of noise except partition noise.

It should be remembered that the conductance G_o of Figs. 677 and 678 is made up of the transferred aerial conductance, the dynamic conductance of the tuned circuit and the transit time conductance; in fact the portions to the left of PQ are a condensed representation of Figs. 674 and 675 respectively. The complete circuits are thus as shown in Figs. 679 and 680.

From Fig. 679 the mean square signal voltage at the grid is :-

$$\overline{s_v^2} = \frac{n^2 \overline{v_s^2} \; tG_r^2}{G^2}, \quad \text{where } G = tG_r + G_d + G_t + G_K$$

$$\ldots\ldots\ldots\ldots\ldots\ldots\ldots\ldots (22),$$

and the mean square noise voltage (Fig.680) is

$$\overline{n_v^2} = \frac{K(tG_r + G_d + 4{\cdot}8\, G_t)}{G^2} + K R_s \frac{(tG_r + G_d + G_t)^2}{G^2} + K R_p$$

$$\ldots\ldots\ldots\ldots\ldots\ldots\ldots\ldots (23).$$

The noise factor is given by :-

$$F = 1 + \frac{G_d}{tG_r} + 4{\cdot}8 \frac{G_t}{tG_r} + \frac{(tG_r + G_d + G_t)^2}{tG_r} \cdot R_s + \frac{G^2}{tG_r} \cdot R_p$$

$$\ldots\ldots\ldots\ldots\ldots\ldots\ldots\ldots (24).$$

Equation (24) shows that the conductance G_K affects the noise factor only by its presence in the total conductance G in the last term, and this term is the one involving the equivalent partition noise resistor R_p.

The curves of Fig. 681 have been calculated for a CV1091 valve at a frequency of 45 Mc/s, the appropriate values being :-

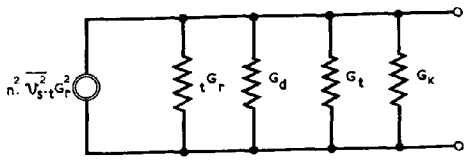

Fig. 679 - Equivalent signal circuit of fig. 674 with addition of conductance due to cathode lead inductance.

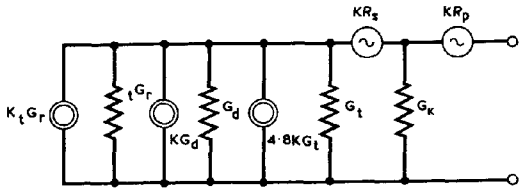

Fig. 680 - Equivalent noise circuit of fig. 675 with addition of noiseless conductance due to cathode lead inductance.

G_d = 0·05 millimho $\qquad$ R_s = 400 ohms

G_t = 0·045 " $\qquad$ R_p = 1100 ohms

G_K = 0·065 " $\qquad$ Total C = 13 pF.

Owing to the increased damping due to G_t and G_K the matched condition is now given by :-

$$tG_r = G_d + G_t + G_K \quad \ldots\ldots\ldots\ldots\ldots\ldots\ldots\ldots\ldots\ldots \quad (25),$$

i.e. tG_r = 0·16 millimho, and the noise factor for this power match is 5·14 db. The minimum noise factor is 4·28 db and this is obtained for tG_r = 0·5 millimho. The band-width at the minimum noise condition is 8·4 Mc/s and this should be compared with the simple case of Fig. 673. The wider band is mainly due to the increased tG_r needed to give minimum noise factor, but is also partly due to the greater damping caused by the finite input conductance of the valve.

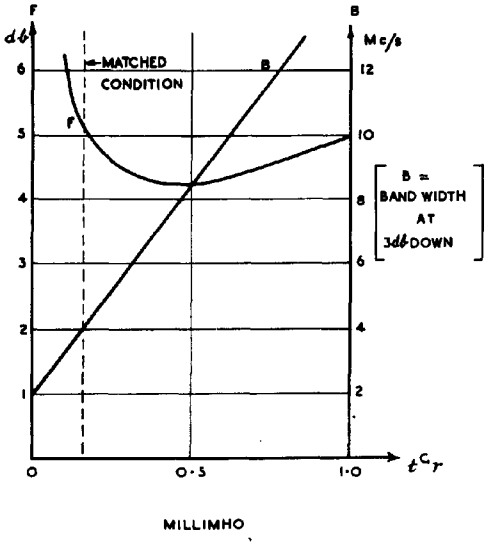

Fig. 681 - Noise factor and bandwidth of circuit of fig. 669 including effects of transit time and cathode lead inductance.

13. Operation at Higher Frequencies

The input conductances due to transit time and the inductance of the cathode lead both vary as the square of the frequency so that if this frequency is increased from 45 Mc/s to, say, 180 Mc/s,

both conductances are increased by a factor of 16. G_t at this new frequency thus becomes 0·72 millimho and G_K 1·04 millimho. Assuming that it is possible by suitable circuit construction to keep the dynamic conductance of the tuned circuit at about the same value although the frequency is increased, this dynamic conductance will be so much less than the input conductance of the valve at 180 Mc/s. that it will have little effect on the noise factor and bandwidth.

If (24) is differentiated and the result equated to zero the transferred aerial conductance for minimum noise factor is found to be :-

$$ {}_tG_r{}^2 = \frac{(G_t + G_d)^2 R_s + (G_t + G_d + G_K)^2 R_p + 4{\cdot}8\, G_t + G_d}{R_s + R_p} \qquad \ldots\ldots\ldots\ldots\ldots\ldots\ldots\ldots (26). $$

Neglecting G_d and using the values for G_t and G_K previously quoted, viz: 0·72 and 1·04 millimhos respectively, the optimum value of ${}_tG_r$ is 2·14 millimhos and the substitution of this in (24) yields the value 10·8 db for the minimum noise factor. This is about 2 db better than the experimental figure for the CV1091 at 200 Mc/s.

It is possible to calculate the contribution of partition noise to the noise factor. If it were practicable to eliminate partition noise, Rp would be zero in (24) and (26) and the optimum values of ${}_tG_r$ and F would then become 3·1 millimhos and 6·0 db respectively. Partition noise is thus responsible for a 5·8 db loss in signal/noise, i.e. a virtual waste of 74% of the transmitter power. This fact leads to two possible lines of development: (i) the redesign of the pentode to reduce the partition noise as much as possible; (ii) the use of a suitable triode as a RF amplifier instead of a pentode.

Considering the first alternative: the high noise factor of the pentode is due to two interdependent causes: (1) the presence of partition noise; (2) the negative feedback due to inductance of the cathode lead which favours partition noise. In the CV1136, the CV1091 type of construction has been retained but the cathode is taken to four pins in the base instead of one. Each of these multiple cathode leads has about the same inductance as the single lead of the CV1091 so that the effective cathode lead inductance is only about one quarter. At the same time the screen current is reduced by aligning the grid and screen wires, thus reducing the partition noise; (see Chap. 15 Sec. 9). The equivalent partition noise resistance is thereby reduced to about 500 ohms instead of 1100 ohms for the CV1091. In practice, however, the CV1136 does not give the improvement in noise factor to be expected theoretically. Measurements have shown that the input conductances of the two valves are not substantially different, and the improvement, which is about 1 db at 45 Mc/s and 2 db at 180 Mc/s, is largely due to the reduction in partition noise. These are average values, and owing to production tolerances it is not unusual to find a particular CV1091 which gives a lower noise factor than a particular CV1136.

At frequencies of the order of 200 Mc/s the inductances of the screen and grid leads become important; the inductance of the latter, for example, is approaching series resonance with the grid-cathode capacitance so that the input impedance of the valve as seen from the pins is lower than that actually present at the electrodes. The simple circuit of Fig. 669 thus needs to be replaced by a fairly complicated network and the noise factor is no longer amenable to easy calculation. This accounts for the discrepancy of about 2 db between the calculated and measured noise factors of the CV1091 at 180 - 200 Mc/s and also, possibly, for the relatively small difference between the CV1091 and CV1136.

The presence of the screen lead inductance means that the screen is losing its effectiveness since its potential may no longer be regarded as constant, and in general the pentode ceases to be a useful amplifier above about 200 Mc/s.

14. The Grounded-Grid Triode

It has already been noted that the elimination of partition noise would bring about a considerable improvement in noise factor. A triode has no partition noise but cannot be used in the conventional grounded-cathode circuit owing to the feedback which would occur through the grid-anode capacitance. If, however, the triode is used in an inverted amplifier or grounded-grid circuit, the grid will, if a suitable valve construction is adopted, act as an electrostatic screen between the input and output circuits (Fig. 682).

It has been shown in Chap. 7 Sec. 20 that the input admittance of such a stage is

$$y_i = \frac{\mu + 1}{R_a + z_\ell}, \quad \ldots\ldots\ldots\ldots\ldots\ldots\ldots\ldots\ldots\ldots (26),$$

where

μ is the amplification factor
R_a is the anode slope resistance
and z_ℓ the load in the anode circuit.

Over the pass band of the amplifier the anode load may be regarded as a pure resistance R_ℓ so that the input admittance is thus a pure conductance of value

$$G_i = \frac{\mu + 1}{R_a + R_\ell} \quad \ldots\ldots(27).$$

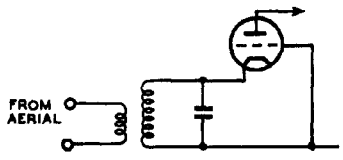

Fig. 682 - Input circuit of grounded-grid stage.

The signal circuit is therefore as shown in Fig. 683 and is the same as Fig. 679 with G_i replacing G_K. A typical value of G_i is 5 millimhos and the effect of this in parallel with the tuned circuit is to produce such heavy damping that bandwidth is no longer a problem.

The shot noise currents flow through the input circuit and thus produce negative feedback voltages across it. These voltages are developed across a resistance so that the mechanism is different from that of the inverse feedback produced by cathode lead inductance in the circuit of Fig. 676. The result is the same, however, and it is found that the equivalent circuit of Fig. 680 is applicable to the grounded grid triode if G_K is replaced by G_i and the partition noise generator omitted (Fig. 684).

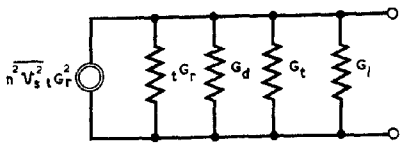

Fig. 683 - Equivalent signal circuit of fig. 682.

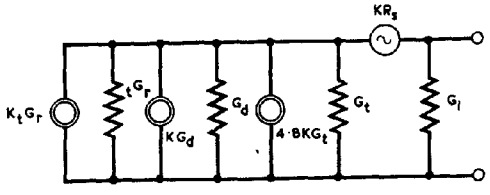

Fig. 684 - Equivalent noise circuit of fig. 682.

The noise factor of the stage is obtained from (24) by putting Rp = 0, and the optimum value of $t^{G}r$ is likewise obtained from (25). This has already been done in the discussion of the contribution of partition noise to the noise factor of a CV1091 at 180 Mc/s. The results were: $t^{G}r$ = 3·1 millimhos and F = 6 db. Thus if the transit time conductance is the same in the two cases (a not unreasonable assumption) a grounded grid triode gives the same noise factor as a pentode without partition noise. The replacement of a pentode by a grounded grid triode at 180 Mc/s would thus lead to an improvement of 5·8 db in signal/noise ratio, in other words, the virtual loss of 74% of the transmitter power would be eliminated.

In all the preceding discussions on noise factor the noise generated in stages other than the first has been neglected. Just as it is possible to represent the shot and partition noise of the first stage by an equivalent noise generator at the grid, even though these are produced in the anode circuit, so it is equally possible to represent all noise generated within the amplifier band-width by subsequent stages by a fictitious noise generated at the first grid. It is merely necessary to assign to this generator a mean square voltage which will produce the same noise power in the output load. The second stage of the amplifier will be the most important so that the mean square voltage of the equivalent noise source at the first grid is defined as KR_2. This generator will be in series with the partition noise generator in Fig. 680 and will replace it in the corresponding equivalent circuit for the grounded grid triode. Fig. 684 is thus modified to Fig. 685 by the addition of this extra noise source.

The exact value to be assigned to R_2 will of course depend on the gain of the first stage as well as the noise generated by the second and following stages. A numerical example will illustrate this and emphasise the difference between a pentode and a grounded grid triode as the first stage. At 45 Mc/s a typical value for R_2 is 10 ohms; in the case of the CV1091 this is in series with the 1100 ohms partition noise generator and is thus merely equivalent to increasing the latter by about 1%, an entirely negligible amount. On the other hand, in the grounded grid triode the signal and noise generated in the first stage are so reduced by the high degree of negative feedback that noise generated in the second stage begins to become important.

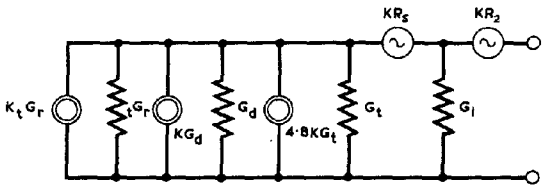

Fig. 685 - Modification of fig. 684 by the addition of equivalent noise generator for subsequent stages.

Re-writing equations (24) and (26) for the grounded-grid triode we obtain :-

$$F = 1 + \frac{G_d}{t^{G}r} + 4{\cdot}8\,\frac{G_t}{t^{G}r} + \frac{(t^{G}r + G_d + G_t)^2}{t^{G}r} \cdot R_s + \frac{G^2}{t^{G}r} \cdot R_2 \qquad \ldots\ldots\ldots\ldots\ldots (28),$$

where $G = t^{G}r + G_d + G_t + G_i$,

$$\text{and } {}_tG_r^2 = \frac{(G_t + G_d)^2 R_s + (G_t + G_d + G_i)^2 R_2 + 4{\cdot}8\, G_t + G_d}{R_s + R_2} \quad \ldots\ldots (29).$$

The low value of R_2 is to a large extent offset by the high value of G_i occurring in its coefficient. The variation of F with ${}_tG_r$ is plotted in Fig. 686 for the two cases $R_2 = 0$ and $R_2 = 10$ ohms, the other values being:-

G_d = 0·05 millimho

G_t = 0·05 millimho

G_i = 5 millimhos.

These are typical of the CV66 which is similar to the CV1091 and CV1136 in external appearance.

Referring to Fig. 686, owing to the high input conductance at the cathode the value of ${}_tG_r$ for the matched condition is 5·1 millimhos and it is essential to have a considerably smaller value than this for minimum noise factor. This should be compared with Fig. 681 for the CV1091. The improvement in noise factor between the CV66 and CV1091 is almost exactly 1 db; without the noise produced by the second stage the improvement would be 0·75 db greater.

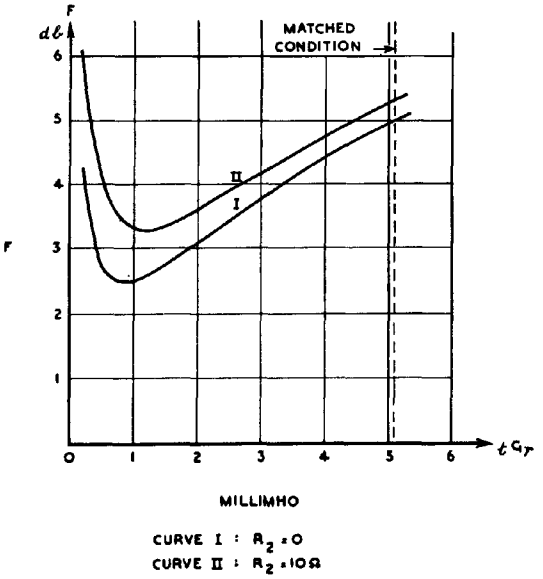

Fig. 686 - Variation of noise factor of circuit of fig. 682 with transferred aerial conductance.

As the frequency of operation is increased all stages of the amplifier become more noisy, so that not only does G_v increase but R_2 also. It is therefore not to be expected that a grounded grid triode will ever give a performance comparable with the theoretical pentode without partition noise. At 180 Mc/s the CV66 has a noise factor of about 7 db compared with 10.8 db and 6 db calculated for the CV1091 with and without partition noise respectively. At frequencies of the order of 600 Mc/s it is no longer possible to think of valve and circuit as separate entities; they must be designed together as a composite whole and every effort must be made to keep the electrode clearances to an absolute minimum in order to prevent transit time noise rising to an inordinate value. It should be remembered that the transit time conductance for any given valve increases by nearly 200 times between 45 Mc/s and 600 Mc/s. Valves such as the CV88 and CV153 which are grounded-grid triodes specially designed for high frequencing working give noise factors of about 10 db at 600 Mc/s. Typical curves illustrating the variation in minimum noise factor with operating frequency for four valves are shown in Fig. 687. The circuit arrangements for different frequencies and the noise factor of the receiver as a whole are further discussed in Sec. 31.

FREQUENCY CONVERSION (MIXING)

15. General

Some reasons for employing the super-heterodyne principle in radar receivers are given in Sec. 5. These may be restated and amplified as follows :-

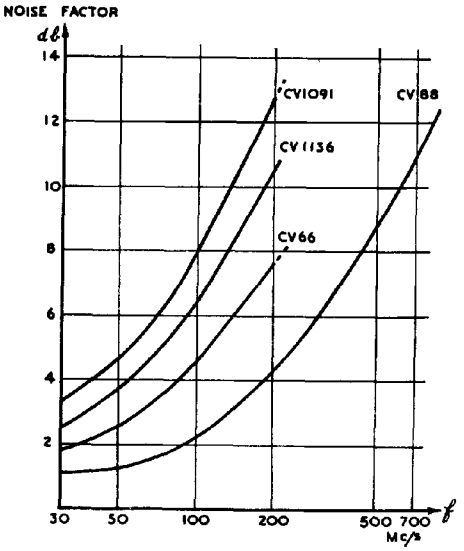

Fig. 687 - Variation of noise factor with operating frequency.

(i) When centimetre waves are employed no useful signal frequency amplification is possible so that there is no alternative to the super-heterodyne principle, and the mixer must of necessity be the first stage in the receiver.

(ii) It is much easier to obtain the necessary pass band characteristics if the amplification takes place in a fixed frequency or pre-tuned amplifier. This is normal communications technique but there is an even greater necessity for maintaining constant amplifier performance in radar reception (see Sec. 37).

(iii) The problem of selectivity, so important in communications work , is considerably simplified by conversion of the signal to a lower "intermediate" frequency. However, in radar the question of distinguishing between two closely separated signal frequencies does not normally arise. Such interference as is experienced in radar working is usually of a different nature and is not dealt with in this chapter.

The higher the carrier frequency the greater the problem of obtaining amplification while maintaining stability. From this point of view it is advantageous to introduce the frequency converter at the earliest possible point in the receiver. However, the actual position occupied by the converter or "mixer" has to be considered from the point of view of obtaining the maximum signal/noise ratio in the receiver as a whole; (see Sec. 2).

It is intended to deal here with the basic principles of frequency conversion within the frequency range in which conventional valve structures (e.g. pentode, hexode) are used. Great detail will not

be entered into since such frequency converters have no extensive radar application and the subject is dealt with in many standard works. It does, however, form a useful introduction to the basic principles of the Two-Pole Converter (diode, crystal) which can be used at much higher frequencies. Neither pentode nor hexode mixers are commonly employed in Service radar receivers operating on a radio frequency higher than 50 Mc/s, since they are too noisy to use unless many stages of RF amplification have preceded the mixer stage. Triodes are usable as single-input mixers at frequencies up to about 200 Mc/s, but because of their large input capacitance they are replaced at higher frequencies by diodes. Diode mixers are commonly used for signal frequencies from 50 Mc/s - 500 Mc/s. The input capacitance and cathode lead inductance of diodes prohibits their use in the centimetre band; neither can be reduced indefinitely while sufficient emission is maintained, and ultimately crystal mixers must be employed. Although these are relatively inefficient frequency converters they are the only type which present sufficiently small input capacitance to the RF signal while still possessing a workable value of conversion efficiency.

16. Fundamental Principle of Frequency Conversion

The underlying principle of frequency conversion is to feed into the mixer (a) the incoming signal and (b) an output from an unmodulated Local Oscillator, i.e., an oscillator situated in the receiver. The output from the mixer contains a number of frequencies one of which is the required intermediate frequency.

In order to introduce into the output voltage or current frequencies which are not present in the input, the mixer must be a device which is effectively non-linear. For example, suppose that the signal voltage v_s applied to the mixer may be represented by :-

$$v_s = \hat{v}_s \cos\omega_s t \quad \ldots\ldots\ldots\ldots\ldots\ldots\ldots\ldots\ldots\ldots (1),$$

and that the local oscillator voltage v_o is given by

$$v_o = \hat{v}_o \cos\omega_o t \quad \ldots\ldots\ldots\ldots\ldots\ldots\ldots\ldots\ldots\ldots (2).$$

If these are added together the result is

$$v = v_s + v_o = \hat{v}_s \cos\omega_s t + \hat{v}_o \cos\omega_o t \ldots\ldots (3),$$

which is the voltage that would result if the signal and local oscillator output were applied in series to the mixer. Now let a resultant current i flow in the mixer output circuit as a result of the voltage v at the input; then if the mixer is linear,

$$i = b_1 v \quad (\text{where } b_1 \text{ is a constant}) \ldots\ldots\ldots\ldots\ldots\ldots (4)$$

$$\text{or} \qquad i = b_1 \hat{v}_s \cos\omega_s t + b_1 \hat{v}_o \cos\omega_o t \quad \ldots\ldots\ldots\ldots\ldots (5),$$

showing that the output contains components of two frequencies only, namely, the signal and local oscillator frequencies, no new frequency having been produced.

The simplest non-linear case that may be considered is the addition of a term involving v^2 to (4), i.e.

$$i = b_1 v + b_2 v^2 \quad (\text{where } b_2 \text{ is a constant}) \ldots\ldots\ldots (6).$$

Substituting from (3), we obtain

$$i = b_1 (\hat{v}_s \cos\omega_s t + \hat{v}_o \cos\omega_o t) + b_2 (\hat{v}_s \cos\omega_s t + \hat{v}_o \cos\omega_o t)^2$$

and, after expansion, this may be put in the form

$$i = b_1 \hat{v}_s \cos\omega_s t + b_1 \hat{v}_o \cos\omega_o t + \frac{1}{2} b_2 (\hat{v}_s^2 + \hat{v}_o^2) + \frac{1}{2} b_2 \hat{v}_s^2 \cos 2\omega_s t + \frac{1}{2} b_2 \hat{v}_o^2 \cos 2\omega_o t + 2 b_2 \hat{v}_s \hat{v}_o \cdot \cos\omega_s t \cdot \cos\omega_o t \quad \ldots\ldots\ldots\ldots\ldots (7).$$

The linear term in (6) gives signal and oscillator frequency components as before. The quadratic term gives rise to :-

(1) a DC component;
(2) second harmonic components of signal and oscillator frequencies;
(3) a product term (the last in (7)) which on further expansion gives
$b_2 \hat{v}_s \hat{v}_o \cos(\omega_s - \omega_o)t + b_2 \hat{v}_s \hat{v}_o \cos(\omega_s + \omega_o) t$,

and therefore represents components of two new frequencies, which are respectively equal to the difference and sum of the signal and oscillator frequencies. (1) and (2) might have been expected, since a non-linear device is to some extent a rectifier, while operation on a curved characteristic always gives rise to harmonics. The terms involved in (3) are those fundamental to the frequency-changing process, the difference term usually being chosen for IF amplification. If equation (6) is extended further to include terms of higher order in v, viz :-

$$v = b_1 v + b_2 v^2 + b_3 v^3 + b_4 v^4 + \ldots\ldots , \ldots\ldots\ldots (8)$$

the output current will include not only signal and oscillator frequencies and their second harmonics but also a whole series of "mixing" components of angular frequencies $\pm (m\omega_s \pm n\omega_o)$ where m and n may take independently any integral values from zero upwards. If the signal is of very small amplitude compared with the local oscillator input (i.e. $\hat{v}_o \gg \hat{v}_s$) the only mixing components of appreciable amplitude are those for which m = 1, i.e. those of angular frequencies $\pm (\omega_s \pm n\omega_o)$. n = 1 gives the sum and difference frequencies which can be called "first order" mixing components, while the frequencies for which n = 2, n = 3, etc., may be called "second order", "third order", etc., respectively.

For a signal frequency f_s, local oscillator frequency f_o, and intermediate frequency f_i there is thus a general relation,

$$f_s \pm n f_o = \pm f_i$$

giving

$$f_o = \frac{f_s \pm f_i}{n} \quad \ldots\ldots\ldots\ldots\ldots\ldots (9).$$

Thus for a signal frequency of 200 Mc/s and an IF of 45 Mc/s possible values for f_o are :-

(a) 155 or 245 Mc/s (1st order mixing);
(b) 77·5 or 122·5 Mc/s (2nd order mixing);
(c) 51·7 or 81·7 Mc/s (3rd order mixing);

etc.

So far nothing has been said about the relative efficiencies of the different orders of mixing. This will depend upon the characteristic of the mixer, but in general it may be said that the efficiency falls off considerably with increasing order. (The efficiency can be roughly defined here as the IF output current for a given signal voltage input.) In practice therefore it is usual to employ first order mixing, although in some cases higher orders are used. For example, it may not be convenient to use an oscillator with a sufficiently high fundamental frequency to make first order mixing possible. Alternatively the LO frequency might be reduced in order to provide a wide tuning range, since the change in frequency of the nth harmonic is n times the change in the fundamental frequency. (A relatively wide tuning range is more easily obtained at lower frequencies, since the effects of stray capacitance, lead inductance, etc. are less important.)

Non-linear devices are readily available in the triode, pentode or hexode which have curved mutual characteristics. The analysis of frequency conversion with such devices is comparatively straightforward provided that it is assumed that the input impedance is infinite and that there is no coupling or interaction between input and output circuits. The inherent difficulties of the problem of the two-pole converter arise from the fact that in this case these assumptions are no longer valid.

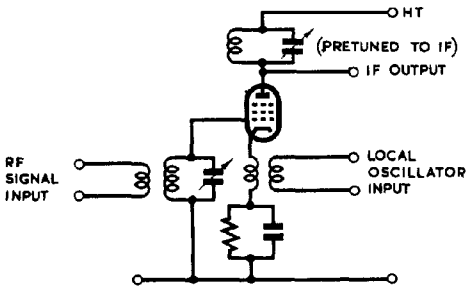

Fig. 688 - Pentode as single input mixer.

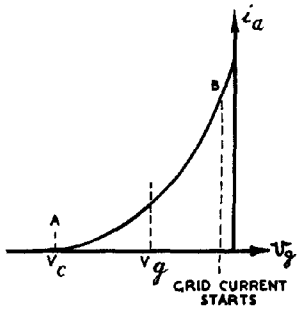

Fig. 689 - Mutual characteristic of pentode of fig. 688.

17. The Single-Input Mixer

A simple frequency converter (sometimes known as a Single-Input Mixer) using a pentode is shown in Fig. 688. The term Single Input is used to denote the application of both signal and oscillator voltages effectively in series between the cathode and one other electrode, in this case the control grid. The mutual characteristic is shown in Fig. 689 and it is assumed that the working point never runs the valve into grid current nor beyond cut-off, i.e. it always lies between A and B on the characteristic.

The analysis is simple if it is assumed that the characteristic between A and B is parabolic, so that the anode current for any given value of grid-cathode voltage v_g is given by :-

$$i_a = k_o (v_g - V_c)^2 \quad \ldots\ldots\ldots\ldots\ldots\ldots\ldots\ldots (10)$$

where V_c is the cut-off voltage. Bias of value V_g is applied to the valve so as to bring the mean position of the working point about half way between A and B. The instantaneous grid voltage is then

$$v_g = V_g + \hat{v}_s \cos\omega_s t + \hat{v}_o \cos\omega_o t \quad \ldots\ldots\ldots\ldots (11).$$

It is convenient to write

$$v_g = V_g + v \quad \ldots\ldots\ldots\ldots\ldots\ldots\ldots\ldots\ldots\ldots (12)$$

where $$v = \hat{v}_s \cos\omega_s t + \hat{v}_o \cos\omega_o t \quad \ldots\ldots\ldots\ldots\ldots (13),$$

and if $V_g + v$ is substituted for v_g in (10) the result may be written in the form :-

$$i_a = b_o + b_1 v + b_2 v^2 \quad \ldots\ldots\ldots\ldots\ldots\ldots\ldots (14).$$

Equation (13) is identical with (3) while (14) differs from (6) only by the presence of the constant term b_o, representing the direct current at the bias point. The resultant anode current is therefore obtained from (7) merely by adding b_o to the right hand side, and as before the anode current contains first order mixing components. Since the anode load presents an appreciable impedance at one frequency only, in this case the difference frequency, the voltage developed at the anode consists almost entirely of the component at this frequency.

A useful concept in mixers using valves of the conventional type is the Conversion Conductance G_c which is defined as :-

$$G_c = \frac{\text{peak value of IF current in anode circuit}}{\text{peak value of signal voltage applied to the valve}}.$$

This corresponds to the mutual conductance when the valve is used as a straight amplifier. Comparison of (10) and (14) shows that $b_2 = k$ while the amplitude of the IF component is $b_2 \hat{v}_s \hat{v}_o$ so that the conversion conductance is

$$G_c = k_o \hat{v}_o \quad \ldots\ldots\ldots\ldots\ldots\ldots\ldots\ldots\ldots\ldots (15).$$

Clearly the best conversion is obtained when the oscillator input voltage is the maximum possible which, if the working point is not to move beyond the limits AB, is, $V_g - V_c$, so that the maximum possible conversion conductance under these conditions is

$$G_c = k_o (V_g - V_c) \quad \ldots\ldots\ldots\ldots\ldots\ldots\ldots\ldots (16).$$

From (10) the mutual conductance G_m at the bias point is

$$G_m = 2k_o (V_g - V_c) \quad \ldots\ldots\ldots\ldots\ldots\ldots\ldots\ldots (17),$$

so that the process of conversion has only half the voltage efficiency of straight amplification. The figure of one-half naturally holds only for a parabolic characteristic under the stated operating conditions, but the general result is true for any single-input mixer, namely, that G_c is always less than G_m for the same valve and the same mean anode current.

In practice the mutual characteristic is not parabolic, also the working point may move beyond cut-off, so that the relation between i_a and v involves terms of higher degree than the second, viz :-

$$i_a = b_0 + b_1 v + b_2 v^2 + b_3 v^3 + b_4 v^4 + \ldots\ldots, \ldots\ldots\ldots \quad (18).$$

Under these conditions higher order mixing components are present in the anode circuit.

The disadvantages of single-input mixers are well known. The oscillator voltage must be sufficient to swing the working point between the limits of the mutual characteristic otherwise conversion is inefficient. If the limits are exceeded grid current flows and damps the signal input circuit; hence the local oscillator input voltage is critical. Coupling may occur between the signal and oscillator circuits through the grid-cathode capacitance, causing interaction between the two tuning controls. The use of a multi-electrode valve with independent application of the signal and local oscillation to separate grids which are electrostatically screened from each other minimises this objectionable tendency as well as eliminating any chance of grid current damping the signal circuit. Such a system may be referred to as a Double-Input Mixer.

18. The Double-Input Mixer

An example of a double-input mixer is shown in Fig. 690. The signal is usually fed to the first grid and the local oscillation to the third; in some mixers these feeds are interchanged.

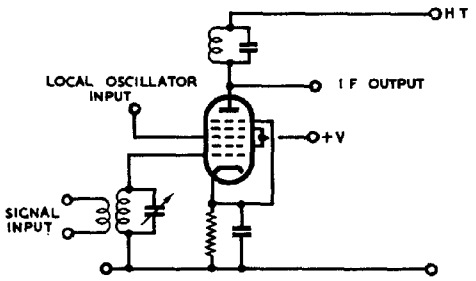

Fig. 690 - Typical double-input mixer circuit.

In considering the operation of this mixer it is essential to examine the implications of the term "effectively non-linear". The mixing action does not depend on curvature of the mutual characteristics connecting anode current with either first grid voltage (v_1) or third grid voltage (v_3). These may be ideally represented by straight lines; (Fig. 691). If instead of the one characteristic of Fig. 691(a), a set is taken for different values of third grid voltage, the results are approximately as shown in Fig. 692. The characteristics are all straight lines with a common cut-off voltage but their slope depends on the voltage applied to the third grid. It is thus possible to write

$$i_a = G_1 (v_1 - {}_1V_c) \ldots\ldots\ldots\ldots\ldots\ldots\ldots \quad (19),$$

where G_1, the mutual conductance referred to the first grid, is a parameter depending on v_3, and ${}_1V_c$ is the cut-off voltage. The simplest variation in G_1 which may be considered is linear, i.e.

$$G_1 = A (v_3 - {}_3V_c) \ldots (20)$$

which combined with (19) gives

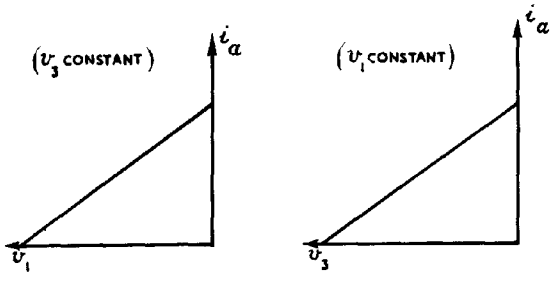

Fig. 691 - Ideal mutual characteristics of double-input mixer.

$$i_a = A (v_1 - {}_1V_c) (v_3 - {}_3V_c) \ldots\ldots\ldots\ldots\ldots\ldots \quad (21).$$

Setting v_3 and v_1 constant in turn will give the linear relations expressed graphically in Figs. 691 (a) and (b). Both first and third grids carry bias in addition to their respective oscillatory inputs, so that :-

$$v_3 = V_3 + \hat{v}_o \cos\omega_o t \quad \ldots\ldots\ldots\ldots\ldots\ldots\ldots\ldots\ldots (22),$$

with a corresponding equation for v_1.

Substitution in (21) and subsequent rearrangement yields the equation for the anode current in the form :-

$$i_a = a_1 + a_2 \hat{v}_s \cos\omega_s t + a_3 \hat{v}_o \cos\omega_o t + a_4 \hat{v}_o \hat{v}_s \cos\omega_s t \cos\omega_o t$$
$$\ldots\ldots\ldots\ldots\ldots\ldots\ldots (23).$$

The last term of this equation gives rise to the two first order mixing terms :-

$$\frac{1}{2} a_4 \hat{v}_s \hat{v}_o \cos(\omega_s - \omega_o) t + \frac{1}{2} a_4 \hat{v}_s \hat{v}_o \cos(\omega_s + \omega_o) t \ldots\ldots (24).$$

Thus, although both mutual characteristics are linear, frequency changing occurs.

There is no paradox in this. With a single input mixer there are two variables only, i_a and v_g, and the relation between them is represented by a curve drawn in two dimensions, i.e. the mutual characteristic. If this characteristic is straight, no frequency conversion occurs; if it is curved, frequency conversion takes place. In the case of a double-input mixer three variables are involved, i_a, v_1 and v_3, and the relation between them can be expressed by a three-dimensional graph, i.e. a surface. The equation of this surface is that of (21), and although lines drawn on it for constant values of v_1 and v_3 are straight the surface itself is curved. If the surface were plane, equation (21) would be replaced by one of the form:-

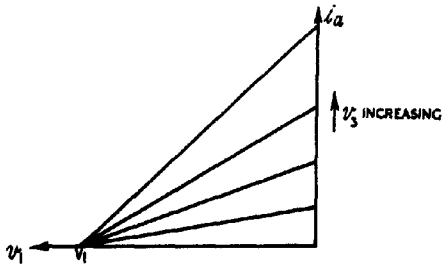

Fig. 692 - Variation of $i_a - v_1$ characteristic with v_3.

$$i_a = p + q v_1 + r v_3 \quad \ldots\ldots\ldots\ldots\ldots\ldots\ldots\ldots (25),$$

which would give no frequency-changing components. The term "non-linear" as applied to a characteristic should thus be used in its more general sense when double-input mixers are considered.

The mutual conductance G_1 referred to the first grid may be defined as the partial differential coefficient $\frac{\partial i_a}{\partial v_1}$ (v_3 constant) and partial differentiation of the planar characteristic equation (25) gives

$$G_1 = q = \text{constant} \quad \ldots\ldots\ldots\ldots\ldots\ldots\ldots\ldots (26).$$

Differentiation of (21) will of course give (20) which expresses the variation of slope G_1 with v_3. Thus it may be said that for frequency conversion to take place the mutual conductance G_1 must be varied at the

oscillator frequency. That this applies equally well to the single-input mixer can be seen from Fig. 689 where the working point swings at the oscillator frequency between the limits A and B, i.e. between one point where the mutual conductance is low and another where it is high.

From (24) the conversion conductance G_c for the double-input mixer is $\frac{1}{2} a_4 \hat{v}_o$ which again depends on the oscillator amplitude. Under the conditions assumed here the maximum G_c is obtained when the third grid voltage just swings between zero and cut-off. The variation of G_1 with time is then as shown in Fig. 693 and this may be called Class A Operation.

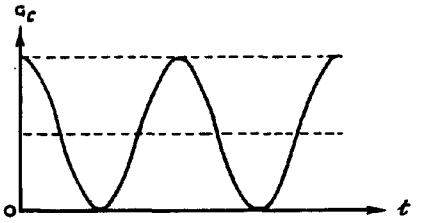

Fig. 693 - Class A operation of double input mixer.

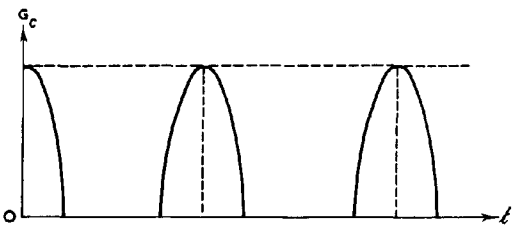

Fig. 694 - Class C operation of double-input mixer.

It is found that a larger conversion conductance can be secured if the valve is driven beyond third grid cut-off during the oscillator cycle. This may be called Class C Operation, and is illustrated in Fig. 694. In this case the variation of G_1 with time is no longer sinusoidal, but since it is periodic at the oscillator frequency it may be expressed as a Fourier series :-

$$G_1 = g_o + g_1 \cos\omega_o t + g_2 \cos 2\omega_o t + g_3 \cos 3\omega_o t + \ldots \quad \ldots(27).$$

With this substitution, (19) becomes

$$i_a = (g_o + g_1 \cos\omega_o t + g_2 \cos 2\omega_o t + g_3 \cos 3\omega_o t + \ldots\ldots)$$
$$(V_1 - {}_1V_c + \hat{v}_s \cos\omega_s t) \ldots\ldots\ldots\ldots \quad (28),$$

where V_1 is the bias on the first grid. When (28) is expanded it contains product terms of the form :-

$$g_n \hat{v}_s \cos\omega_s t \cdot \cos n\omega_o t; \quad (n = 1, 2, 3, \text{etc.}).$$

n = 1 will give the first order mixing components, n = 2 the second order and so on. With n = 1 the conversion conductance for first order mixing is found to be :-

$$G_c = \frac{1}{2} g_1 \quad \ldots\ldots\ldots\ldots\ldots\ldots\ldots\ldots\ldots\ldots \quad (29).$$

The value of g_1 depends on the bias and the amplitude of the oscillator voltage applied to the third grid. If this bias is obtained by clamping at this grid (see Chap. 12), so that the third grid voltage never rises appreciably above zero, the first order conversion conductance varies with the amplitude of the oscillator voltage in the manner shown in Fig. 695.

For increasingly higher orders of mixing the conversion conductance falls off rapidly unless the oscillator voltage is of very large amplitude. Measurements taken under typical operating conditions with a reasonable value of oscillator voltage gave relative values of 12, 6 and 1 for the conversion conductances for first, second and third order mixing respectively.

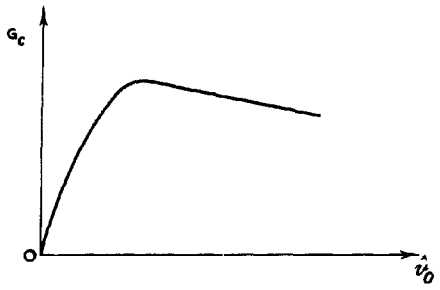

Fig.695. First order mixing : variation of conversion conductance with amplitude of oscillator voltage.

19. The Two-Pole Converter

Conventional frequency converters are not in general suitable for radar equipments operating at signal frequencies above about 200 Mc/s. For conversion at these frequencies the conversion element is a diode or a crystal; i.e. a two-pole converter.

The problem of analysis of the two-pole converter is considerably complicated by the fact that the signal frequency input, local oscillator input, converter element and IF output load are all in series. There may also be a steady voltage source in the circuit to provide bias; this is shown as a battery in the basic circuit of Fig. 696. The assumption of independence of input and output no longer holds, but in order to reduce the problem to manageable proportions it is necessary to make certain simplifications, namely :-

(1) the signal is derived from a circuit the impedance of which is zero at all frequencies not close to the signal frequency, where it may be regarded as resistive;

(2) the impedance of the IF circuit is similarly resistive close to the intermediate frequency and zero for all other frequencies;

(3) the effective local oscillator voltage is assumed to be injected from a source of negligible impedance at all frequencies;

(4) the amplitude of the applied local oscillator voltage is very much greater than the amplitude of either the signal or IF voltages;

(5) the susceptance of the converter element is zero.

The above assumptions naturally limit the general application of the analysis, but to a first approximation they appear to give a satisfactory explanation of the conversion process. The equivalent circuit is shown in Fig. 697; it should be remembered that R_s exists only for the signal frequency and R_i only for the intermediate frequency.

Suppose that the oscillator voltage is applied without any signal; then there will be no voltage drop across R_s, which is effective at the signal frequency only. Since there is no signal input no IF

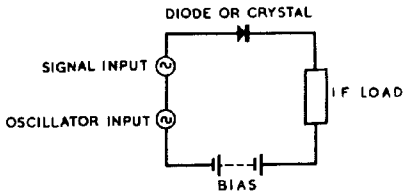

Fig. 696 – Basic circuit of two-pole converter.

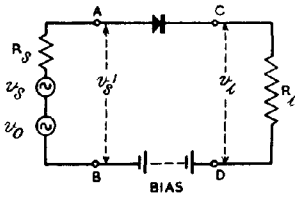

Fig. 697 – Equivalent circuit of two-pole converter.

component is present in the circuit so that no voltage is developed across R_i. The waveform of the current through the converter element is then obtained by the usual construction of Fig. 698. One cycle only is shown in this figure; several cycles are drawn in Fig. 699. If the equation of the converter characteristic is :-

$$i_a = f(v) \quad \ldots\ldots\ldots\ldots\ldots\ldots\ldots\ldots\ldots\ldots\ldots\ldots\ldots\ldots \quad (30),$$

and the voltage v at any instant is

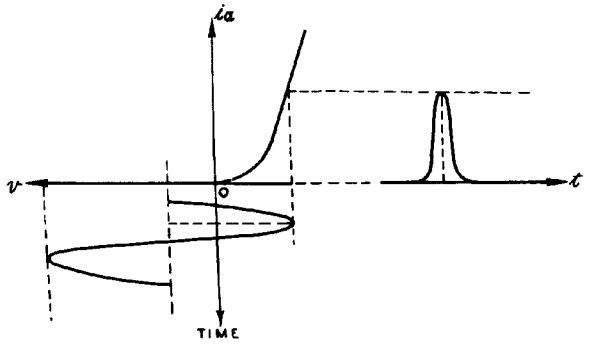

Fig. 698 – Current pulse in converter circuit when oscillator voltage and bias only are applied (one cycle only shown).

$$v = V_o + \hat{v}_o \cos\omega_o t \quad \ldots\ldots\ldots\ldots\ldots\ldots\ldots\ldots\ldots\ldots\ldots\ldots \quad (31),$$

the instantaneous current is

$$i_a = f(V_o + \hat{v}_o \cos\omega_o t) \quad \ldots\ldots\ldots\ldots\ldots\ldots\ldots\ldots \quad (32).$$

This is the equation of the current waveform of Fig. 699(a) and can be expressed in the form of a Fourier series :-

$$i_a = I_o + I_1 \cos\omega_o t + I_2 \cos 2\omega_o t + I_3 \cos 3\omega_o t + \ldots\ldots (33),$$

where the coefficients I_o, I_1, I_2 .... etc., can be calculated given the characteristic equation (30) and V_o and $\hat{v}_o$.

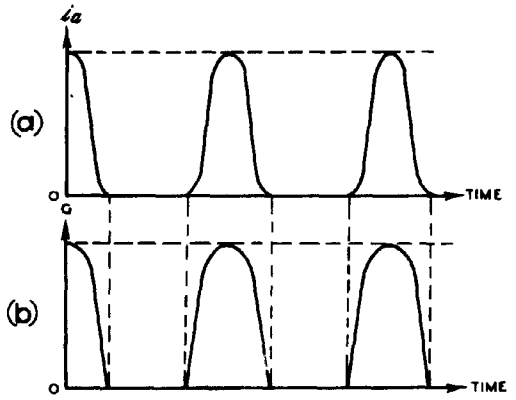

Fig.699 – Variation of current (a) and conductance (b) for two-pole mixer when oscillator voltage and bias only are applied.

The conductance of the converter element is defined as :-

$$G = \frac{di_a}{dv} = f'(v) \quad \ldots\ldots\ldots\ldots\ldots\ldots\ldots\ldots\ldots\ldots \quad (34),$$

and therefore the instantaneous conductance is, from (31) and (34)

$$G = f'(V_o + v_o \cos\omega_o t) \quad \ldots\ldots\ldots\ldots\ldots\ldots \quad (35).$$

This also may be expanded as a Fourier series :-

$$G = G_o + G_1 \cos\omega_o t + G_2 \cos 2\omega_o t + G_3 \cos 3\omega_o t + \ldots\ldots (36).$$

The instantaneous conductance is plotted against time in Fig. 699(b).

It is now necessary to consider what happens when the signal input is applied. Firstly, the signal voltage gives rise to a current in the converter circuit, (Fig. 697), which, since the converter element is a non-linear device, consists of a DC component together with fundamental and harmonic components of the signal frequency. There is a voltage drop across R_s due to the fundamental component only, so that the voltage v_s' actually applied to the converter is of smaller amplitude than the open circuit signal voltage v_s. The applied signal voltage may thus be written :-

$$v_s' = \hat{v}_s' \cos\omega_s t \quad \ldots\ldots\ldots\ldots\ldots\ldots\ldots\ldots\ldots\ldots \quad (37).$$

Secondly, the presence of signal and oscillator voltages implies frequency conversion so that there is an IF component in the circuit which produces a voltage across R_i. Let this voltage be v_i so that :-

$$v_i = \hat{v}_i \cos\omega_i t \quad \ldots\ldots\ldots\ldots\ldots\ldots\ldots\ldots\ldots \quad (38).$$

The difference δv between the instantaneous voltage applied to the converter in the signal and no-signal conditions is thus :-

$$\delta v = \hat{v}_s' \cos\omega_s t - \hat{v}_i \cos\omega_i t \quad \ldots\ldots\ldots\ldots\ldots \quad (39).$$

When the instantaneous voltage is altered by a small amount δv the resultant change in current δi_a is from (34) :-

$$\delta i_a = G\delta v \quad \text{.......................................} \quad (40),$$

so that the current when the signal, as well as the oscillator voltage, is applied is

$$i_a = f(v) + G\delta v \quad \text{...............................} \quad (41).$$

$f(v)$, G and δv are given by (33), (35) and (39) respectively; therefore, on substituting, we obtain :-

$$i_a = I_0 + I_1 \cos\omega_o t + I_2 \cos 2\omega_o t + I_3 \cos 3\omega_o t + \text{..............}$$
$$+ (G_0 + G_1 \cos\omega_o t + G_2 \cos 2\omega_o t + G_3 \cos 3\omega_o t + \text{..........})$$
$$(\hat{v}'_s \cos\omega_s t - \hat{v}_i \cos\omega_i t) \quad \text{.............................} \quad (42).$$

If this is expanded, the only terms of interest are those giving the signal frequency and intermediate frequency currents, and for first order mixing these are :-

$$(G_0 + G_1 \cos\omega_o t)(\hat{v}'_s \cos\omega_s t - \hat{v}_i \cos\omega_i t) \quad \text{................} \quad (43).$$

Since $\omega_i = \omega_s - \omega_o$, rearrangement of (43) gives the amplitude i_s of the signal frequency current :-

$$\hat{i}_s = G_o \hat{v}'_s - \frac{1}{2} G_1 \hat{v}_i \quad \text{..............................} \quad (44),$$

and the amplitude $\hat{i}_i$ of the intermediate frequency current :-

$$\hat{i}_i = \frac{1}{2} G_1 \hat{v}'_s - G_o \hat{v}_i \quad \text{...........................} \quad (45).$$

To (44) and (45) must be added a third relation :-

$$\hat{v}_i = R_i \cdot \hat{i}_i \quad \text{.......................................} \quad (46).$$

These three equations enable the performance of the mixer element to be determined completely, but it should be remembered that the simplicity of the relations is apt to be misleading. G_o and G_1 must be obtained by Fourier analysis, and this cannot be done unless the characteristic equation of the element, the bias and the amplitude of the oscillator input are all known. **For nth order mixing it is easy to show that the only difference in (44) and (45) is the substitution of G_n for G_1:**

Despite the mathematical complication of a complete solution, some general results may be obtained. If (44), (45) and (46) are solved for $\hat{i}_s$ and $\hat{i}_i$ the results are :-

$$\hat{i}_s = \left\{ G_o - \frac{1}{4} \frac{G_1^2 R_i}{1 + G_o R_i} \right\} \hat{v}'_s \quad \text{.................} \quad (47)$$

$$\hat{i}_i = \frac{1}{2} \left\{ \frac{G_1}{1 + G_o R_i} \right\} \hat{v}'_s \; ; \quad \text{.....................} \quad (48),$$

but the input impedance of the mixer at the signal frequency, i.e. the impedance seen when "looking in" at AB of Fig. 697 is $\hat{v}'_s/\hat{i}_s$ and this is

given directly by (47). Its value will thus depend on R_i, the load resistance at the intermediate frequency. Similarly it may be shown that the IF output impedance, i.e. the impedance seen "looking back" into CD depends on R_s, the impedance of the signal frequency source. This is implied in (48) where $\hat{i}_i$ is seen to be proportional to v_s' and this in turn depends on the signal frequency voltage drop across R_s.

Although the mixer element is non-linear, equations (44), (45) and (46) are all of the first degree so that it is possible to apply the concept of equivalent circuits to the mixing process. It is important to note that this holds only for small signal inputs (see equation (40)). It is found that the same equivalent circuit holds for both signal and IF, viz, that of Fig. 700; (G_s and G_i are the conductances of the signal and IF circuits respectively). In this circuit the generator v_s must be considered to be at the signal frequency when the input signal current is being calculated and at the intermediate frequency for determining the IF output current. Its magnitude is the same in both cases.

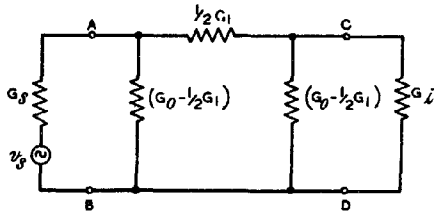

Fig.700.
Equivalent circuit of two-pole mixer.

Since the mixer draws current from the signal source it is preferable to define the conversion process in terms of power. For a given value of $\hat{v}_s$ the IF power delivered to G_1 is a maximum when both G_1 and G_s are equal to the characteristic admittance of the π-section attenuator between AB and CD; (See Chap. 3 Sec. 4). The formula given in Chap. 3 Sec. 7 for the characteristic conductance reduces, after the appropriate change of symbols, to

$$G_s = G_i = \sqrt{G_0^2 - \frac{1}{4} G_1^2} \quad \ldots\ldots\ldots\ldots\ldots\ldots\ldots\ldots \quad (49).$$

This matched condition does not necessarily give the best signal/noise ratio in the receiver, so that a more general approach to the problem is sometimes desirable.

For the signal frequency, the part of the circuit to the right of AB in Fig. 700 may be replaced by a single conductance (G_x) or resistance (R_x) giving the signal frequency equivalent circuit of Fig. 701(a). Similarly, by Thevenin's Theorem, when the IF is being considered the part to the left of CD may be replaced by a generator v_y in series with the output resistance R_y giving the IF equivalent circuit of Fig. 701(b). The peak signal and IF currents in

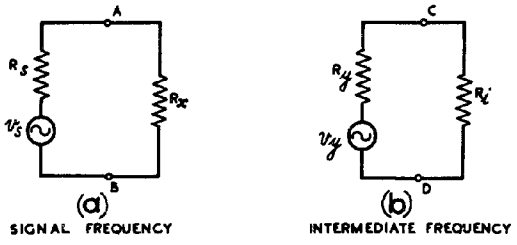

Fig.701.
Equivalent circuits of two-pole mixer.

these two circuits are $\hat{i}_s$ and $\hat{i}_i$ respectively, and the Power Conversion Loss of the mixer may be defined as 10 log A db, where

$$A = \frac{\text{Power in signal frequency equivalent circuit}}{\text{Power in IF equivalent circuit}}$$

$$= \frac{\hat{i}_s^2 \ (R_s + R_x)}{\hat{i}_i^2 \ (R_y + R_i)} \qquad \ldots\ldots\ldots\ldots\ldots\ldots\ldots\ldots\ldots\ldots \ (50).$$

(Several alternative definitions exist, usually implying a matched condition. The definition given above covers all these and has the advantage of being of general application).

The value of A will always be greater than unity but may approach it in certain cases. Referring to Fig. 700, if the conductance $(G_o - \frac{1}{2} G_i)$ of the shunt arms could be reduced to zero then the two equivalent circuits of Fig. 701 would become identical and the power in each would be the same. Unfortunately it is not possible to reduce the difference between G_o and $\frac{1}{2} G_i$ to zero without at the same time making them zero individually so that the series arm of Fig. 700 also becomes zero. There will thus be no IF output unless G_i is also zero, i.e., the dynamic resistance of the IF load circuit must be infinite. Thus, while 100% power conversion is theoretically possible, it is unattainable in practice, the position being analogous to the case of the Class C amplifier, which can theoretically attain 100% efficiency but only if the load impedance in its anode circuit is infinite.

At this point it is convenient to treat the diode and crystal separately, there being important differences between them which will be emphasised by the examination of each in turn.

20. The Diode Mixer

A possible circuit for a diode mixer is shown in Fig. 702. L_1 and C_1 form the anode load of the RF stage and L_1 is tapped for connection to the diode. There is thus a step-down auto-transformer between the RF anode and the diode input. The local oscillation is injected into the tuned circuit through the small capacitance C_2, and it is assumed that the IF is low enough to permit an oscillator voltage of adequate amplitude to be applied to the diode by this means. T is the IF output transformer, C_3 being connected across the primary to bypass the signal and oscillator frequency currents and their harmonics. The battery of Fig. 45 has been replaced by the resistor R_b shunted by C_4, the bias being produced by the mean diode current flowing through R_b.

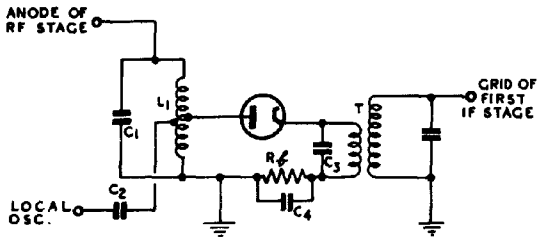

Fig. 702 – Diode mixer circuit.

If the behaviour of this circuit is analysed

it will be found that, for a given input to the grid of the RF stage, maximum voltage at the grid of the first IF is secured when both input and output circuits are matched to the characteristic conductance of the π-section of the equivalent circuit of Fig. 700. The position of the tapping point on L_1 and the turns ratio of the IF transformer T will therefore depend on the value of this characteristic conductance.

As a numerical example of the design considerations the simple case of a linear diode will be examined. The diode may be supposed to have a constant conductance G_+ in the forward direction and zero conductance in the reverse direction. The current waveform of Fig. 699 will then become a succession of peaks of a sine wave while the variation of conductance during the cycle will be represented by a square wave. In Fig. 703 anode current and conductance are shown plotted against the phase angle θ of the oscillator voltage. If the conduction angle of the diode is 2ϕ then all the relevant quantities may be expressed in terms of ϕ as a parameter. The results are :-

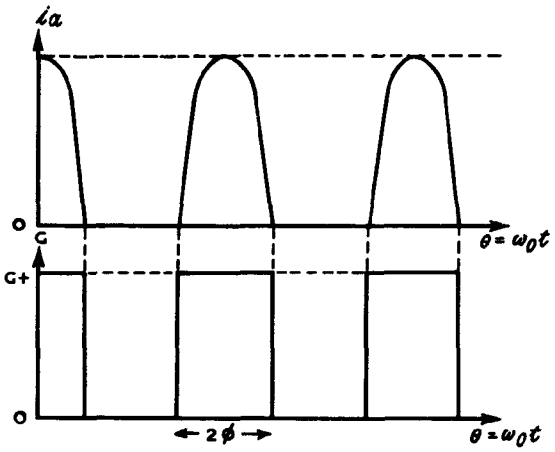

Fig.703-
Modified form of fig. 699 for the case of a linear diode.

$$\text{Mean diode current } \bar{I}_a = \frac{1}{\pi} \hat{v}_o (\sin\phi - \phi\cos\phi) G_+ \quad \ldots\ldots(51).$$

$$\text{Bias voltage} = V_b = R_b \bar{I}_a$$

$$= \hat{v}_o \cos\phi \quad \ldots\ldots(52)$$

$$G_o = \frac{\phi}{\pi} G_+ \quad \ldots\ldots(53)$$

$$G_1 = \frac{2G_+}{\pi} \cdot \sin\phi \quad \ldots\ldots(54)$$

$$G_o - \frac{1}{2} G_1 = \frac{G_+}{\pi} (\phi - \sin\phi) \quad \ldots\ldots(55)$$

$$(G_o^2 - \tfrac{1}{4} G_1^2)^{\frac{1}{2}} = \frac{G_+}{\pi} (\phi^2 - \sin^2\phi)^{\frac{1}{2}} \quad \ldots\ldots(56).$$

These relations apply whether or not the π-section is properly terminated. If in addition this condition is assumed, the four resistances R_s, R_x, R_y and R_i of equation (50) are all equal and the conversion loss-factor A is then simply the ratio of the squares of the signal and IF currents. Dividing (47) by (48) and putting R_i equal to the characteristic resistance, the value of A is found to be :-

$$A = \frac{4\left\{G_o + \sqrt{G_o^2 - \frac{1}{4} G_1^2}\right\}^2}{G_1^2}$$

$$= \frac{\left\{\phi + \sqrt{\phi^2 - \sin^2\phi}\right\}^2}{\sin^2\phi} \quad \ldots\ldots\ldots\ldots\ldots\ldots (57).$$

It follows from (51) and (52) that ϕ is independent of the amplitude $\hat{v}_o$ of the local oscillator voltage and depends only on the bias resistance R_b. This is a natural consequence of the assumption of a linear diode characteristic. The values are tabulated below for two values of ϕ: 30° and 60°, the conductances being given in micromhos.

	$\phi = 30^\circ$	$\phi = 60^\circ$
G_o	333	667
G_1	636	1070
$G_o - \frac{1}{2} G_1$	15	132
$\sqrt{G_o^2 - \frac{1}{4} G_1^2}$	98	345
A	1·84 (2·64 db.)	3·58 (5·54 db.)
R_b	29·2 kΩ	2·3 kΩ

The increase in power conversion efficiency by decreasing the conduction angle 2ϕ from 120° to 60° is well brought out by the above table. At the same time it should be noted that the characteristic conductance has decreased from 345 micromhos to 98 micromhos so that higher impedance circuits are needed to take advantage of the increased efficiency. It may be difficult to design these, particularly the signal frequency circuit, especially if this frequency is high, and this fact, rather than the operating conditions of the diode, may limit the obtainable power conversion efficiency.

When the diode characteristic is non-linear, as it is in practice, the conduction angle is no longer independent of the amplitude of the oscillator voltage and the relations taking the place of equations (51) to (57) are more complicated functions of ϕ. Once the circuit has been designed it is essential to keep the operating conditions constant. If the oscillator input varies, the matching is upset and the efficiency falls off. The easiest quantity to measure is the mean diode current, and a jack is connected in series with the bias resistor R_b so that a meter may be plugged into the circuit. For any given circuit there is a definite mean current, and provision is made for varying the coupling between the oscillator and mixer so that this current can be obtained.

21. The Effect of Diode Capacitance and Lead Inductance

In the foregoing analysis it has been assumed that the diode can be represented by a non-linear conductance, the capacitance between the electrodes being neglected. In a practical diode this capacitance will not be negligible and will become increasingly important as the frequency is raised. There are two effects to be considered. In the circuit of Fig. 702, provided C_3 and C_4 are large compared with the

capacitance of the diode they have very little signal and oscillator voltage developed across them and thus the diode capacitance is of little consequence from the point of view of potential division in the series circuit between the tapping on the RF coil and earth. Hence, this series circuit will, at the signal frequency, be a capacitance practically equal to the capacitance of the diode, and since this is connected across part of the signal circuit it may, if too large, limit the dynamic resistance which may be obtained. This will cause a loss of gain in the RF stage.

A more important effect is that of the inductance of the leads to the diode electrodes, so that, in effect, the valve constitutes a network such as that of Fig. 704. Even if in the circuit of Fig. 702 the leads between the diode and the other circuit components may be made so short that their inductance is negligible, the leads inside the diode bulb are still present. A series resonant circuit may then be set up and the diode will present a low impedance to the tapping on L_1, making it difficult to develop adequate signal voltage at the diode. Reduction of the capacitance of the diode raises the series resonant frequency and extends the useful range of the diode.

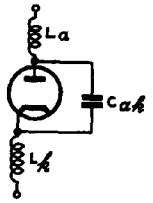

Fig.704.
Effective diode circuit showing lead inductances.

The static characteristic of a diode may be reasonably well represented by the three-halves-power relation :-

$$i_a = k\,(v + b)^{3/2} \quad \ldots\ldots\ldots\ldots\ldots\ldots\ldots\ldots\ldots\ldots \quad (58),$$

where b is a quantity depending upon contact potentials. For a planar diode with negligible initial electron velocities, the constant k is given by :-

$$k = 2{\cdot}34 \,.\, 10^{-6} \,\frac{a}{d^2} \quad \ldots\ldots\ldots\ldots\ldots\ldots\ldots\ldots\ldots\ldots \quad (59)$$

where a = emitting area of the cathode in cm^2,

d = cathode/anode spacing in cm. i_a and v are in amps, and volts respectively.

The capacitance (in pF) is given by :-

$$C_{ak} = 8{\cdot}85 \,.\, 10^{-2} \,.\, \frac{a}{d} \quad \ldots\ldots\ldots\ldots\ldots\ldots\ldots\ldots\ldots\ldots \quad (60).$$

It is important to have as high a value of k as possible since this gives high values of G_o and G_1 and enables the power conversion to be maintained at high frequencies. At the same time, for the reasons stated above, C_{ak} should be kept as small as possible. Comparison of (59) and (60) shows that for a given value of k, halving the spacing between anode and cathode enables the area of the cathode to be reduced to one quarter, C_{ak} thus being halved. The best diode will then be one with a very small spacing and a correspondingly small cathode area. The effect of lead inductance may be overcome by constructing the diode so that it may be built into, and therefore form an integral part of, a coaxial line circuit. A drawing of the CV58 diode, which has been designed on these principles, is shown in Fig. 705.

22. The Crystal Mixer

The crystal "valve", used primarily as a frequency converter for centimetre wavelengths, is shown in section in Fig. 706. The rectifying contact is made by placing a pointed tungsten "whisker" on a smooth silicon surface, the direction of electron flow being from the tungsten to the silicon. During manufacture the position and pressure of the tungsten whisker are adjusted to give a good "front-to-back ratio" and also a specified forward resistance.

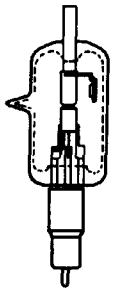

Fig.705 - CV 58 diode.

Finally wax is inserted into the crystal capsule through a hole in the ceramic holder. Its functions are to prevent displacement of the tungsten wire from the silicon and to prevent the ingress of moisture.

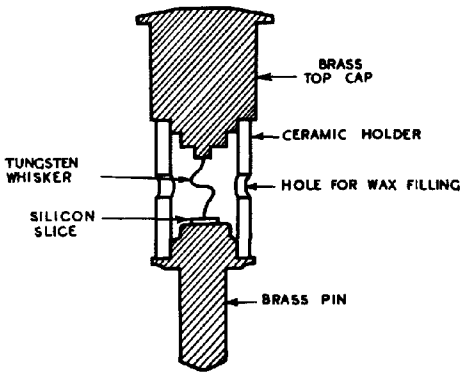

Fig.706 - Section of crystal capsule

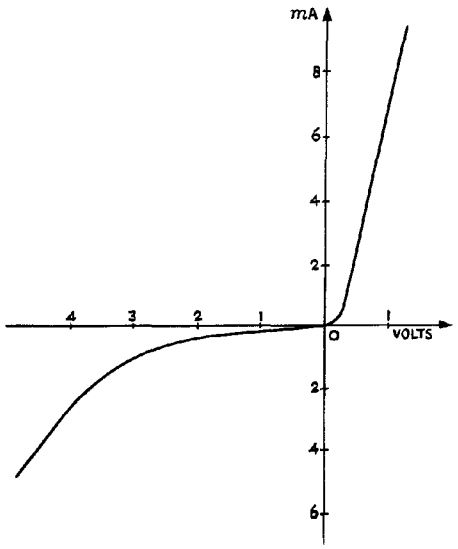

Fig.707 - Static characteristic of crystal.

The static characteristic of a typical crystal is shown in Fig. 707 and the difference between this and the corresponding curve for a diode is at once apparent. The presence of reverse current modifies the current and conductance waveforms of Fig. 699 to those of Fig. 708, the value of G_0, the mean conductance over the oscillator cycle, being increased, while G_1 is decreased. The conductance of the shunt arms of the π-network of Fig. 700 is therefore increased while that of the series arm is decreased, both changes leading to a fall in conversion efficiency. This is particularly so when the oscillator voltage at the crystal exceeds one or two volts, causing the reverse current to increase considerably.

It is therefore to be expected that an optimum oscillator input of fairly small amplitude gives maximum conversion efficiency. In fact it is necessary to use an even smaller oscillator input in order to achieve the optimum signal/noise ratio, so that in practice the maximum conversion efficiency is never reached; (see Sec. 27).

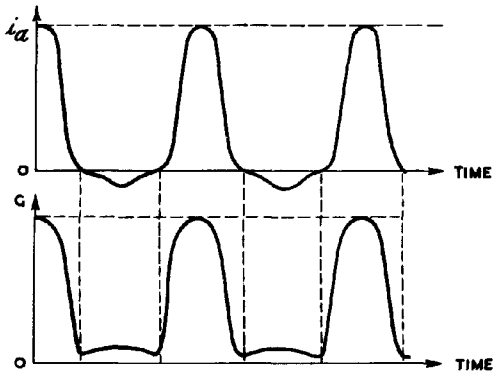

Fig.708_
Modified form of fig. 699 showing effect of reverse current.

Mixer circuits for use with crystals are of two general types, coaxial line and waveguide, and these are shown diagrammatically in Figs. 709 and 710. These designs are made possible by the experimental fact that the resistive component of the RF impedance of the crystal does not vary greatly from one crystal to another. In the coaxial type of mixer circuit the crystal acts as the termination of the line, the stub being connected at a fixed distance from the crystal. The reactive portion can then be tuned out by the stub adjustment so that the input line is correctly terminated. In the waveguide type of mixer

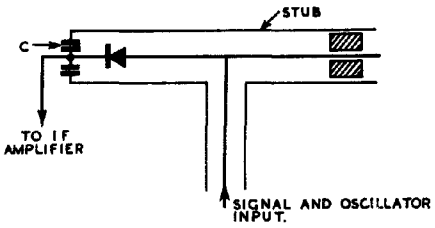

Fig.709_
Diagrammatic sketch of coaxial mixer circuit.

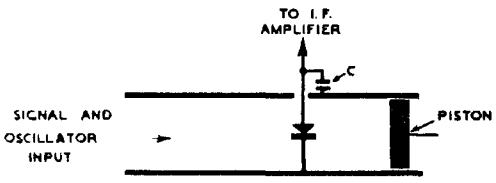

Fig.710_
Diagrammatic sketch of waveguide mixer circuit.

circuit the crystal is placed across the guide parallel to the electric field, the guide dimensions being chosen so that the resistive component of the RF impedance is matched to the wave impedance of the guide. The reactive component is tuned out by adjustment of the piston behind the crystal. The RF by-pass capacitance C is in both cases of the "built-in" type, a dielectric washer or metal flange providing all the capacitance that is required.

It is essential that the match between the crystal and the input line or guide should be as good as possible. Any mismatch causes partial reflection at the termination so that part of the signal energy

is reflected back to the aerial and reradiated, producing a falling-off in performance of the equipment.

23. Effect of Crystal Capacitance

Physical investigations of the phenomenon of crystal rectification indicate the existence of a Boundary Layer of the order of 10^{-6} cm. depth just within the silicon block. This layer is responsible for the rectifying action, as it is only therein that the property of non-linearity occurs. It may be shown that there results an effective capacitance associated with this boundary layer which is termed the Contact Capacitance. The presence of this inherent capacitance in direct association with the rectifying layer limits the high frequency performance to be expected from a crystal mixer.

An equivalent circuit for a crystal is shown in Fig. 711. R_b is the boundary layer resistance which is small in the forward and large in the backward direction, and this is shunted by the boundary layer capacitance C_b. R_s, the Spreading Resistance, is the resistance of the silicon block apart from the boundary layer. R_c includes the resistance of the tungsten whisker and also the contact resistance between the point of the whisker and the upper surface of the boundary layer. L is the inductance of the whisker. The problem of crystal design is thus to keep the value of C_b small without at the same time increasing the total effective series resistance. Development of crystals for higher frequencies proceeds along these lines.

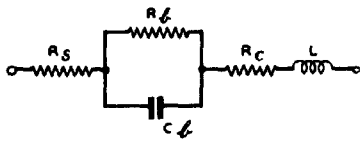

Fig. 711.
Equivalent circuit of crystal.

Owing to the very small contact area necessary to give a reasonably low value of C_b, crystals are easily damaged by overload, which produces heat at the point of contact and destroys the rectification property. Unlike the diode, which recovers from a momentary overload, the crystal is permanently damaged. For this reason great care should be taken in handling crystals; they should not, in particular, be exposed to stray RF fields, but should be kept in a metal box when not in use.

24. Noise in Frequency Converters

In the frequency converter using conventional types of mixing valves (triode, pentode, hexode) the study of noise follows the same lines as that already given for RF amplifiers in Secs. 7-14. With diode mixers the approach is again along similar lines, but owing to the interdependence of input and output circuits the frequency converter and the subsequent IF stage must be considered together as one composite whole. The same is true of crystal mixers with the added complication that the local oscillator contributes to the noise, this contribution becoming increasingly important as the frequency is raised. The various types of frequency converter are considered in turn.

25. Noise in Triode, Pentode and Hexode Mixers

Since the grid and anode circuits of the valve are tuned to widely different frequencies it is possible to use a triode as a frequency converter without instability occurring. The anode load may be taken to be a pure resistance over its pass-band B so that the ratio of signal to noise power in the output of the converter is equal to the ratio of the

mean square signal and noise currents in the anode circuit. These may be represented by equivalent signal and noise generators in the grid circuit as in the case of the RF amplifier, there being only slight modifications to the argument owing to the frequency conversion process. A simple analysis will be given for the shot noise only. The mean square short-circuit noise current in the anode circuit due to shot noise is given by :-

$$i^2 = 2\Gamma^2 . eI_aB \quad \ldots\ldots\ldots\ldots\ldots\ldots\ldots\ldots\ldots\ldots (1)$$

where Γ^2 = space charge reduction factor.

e = electronic charge in colombs.

I_a = anode current in amps.

B = band width in cycles/sec.

In the case of a straight amplifier this noise current may be considered as produced by a fictitious noise generator at the grid of a noiseless valve, the magnitude of the generator voltage being given by

$$\overline{v_n^2} = \frac{2\Gamma^2 e I_a B}{G_m^2} \quad \ldots\ldots\ldots\ldots\ldots\ldots\ldots\ldots (2).$$

In the case of the frequency converter, I_a and Γ^2 both vary at the oscillator frequency and can no longer be treated as constants. The mean square noise current must therefore be obtained by averaging the expression (1) over the oscillator cycle. Although the effective components of the shot noise are those lying within the IF pass band, the fictitious noise generator at the grid may be considered to be at the signal frequency if the mutual conductance G_m is replaced by the conversion conductance G_c. Equation (2) then becomes :-

$$\overline{v_n^2} = \frac{2e B}{G_c^2} \cdot \overline{(\Gamma^2 I_a)} \quad \ldots\ldots\ldots\ldots\ldots\ldots\ldots\ldots (3),$$

and the equivalent shot noise resistance R_s is therefore given by :-

$$R_s = \frac{2e B}{K G_c^2} \cdot \overline{(\Gamma^2 I_a)} \quad \ldots\ldots\ldots\ldots\ldots\ldots\ldots\ldots (4).$$

This can be calculated if the variations of Γ^2 and I_a with grid voltage are known.

The mean square noise current in the anode circuit of a pentode due to both shot and partition noise, is given by :-

$$\overline{i_n^2} = 2e B I_a \left(\frac{I_a + \Gamma^2 I_a}{I_a + I_s}\right) \quad \ldots\ldots\ldots\ldots\ldots\ldots\ldots\ldots (5),$$

where I_s is the screen current. If it is assumed that the ratio of anode to screen currents is constant during the oscillator cycle and equal to m (a not unreasonable assumption) equation (5) then becomes :-

$$\overline{i_n^2} = 2 e B I_a \left(\frac{1 + m\Gamma^2}{1 + m}\right) \quad \ldots\ldots\ldots\ldots\ldots\ldots\ldots\ldots (6).$$

This must be averaged over the oscillator cycle and the result divided by KG_c^2 to give the equivalent noise resistance R_e.

Equation (6) may be re-written

$$\overline{i_n^2} = 2 e B I \left\{ \frac{m (1 + m\Gamma^2)}{(1 + m)^2} \right\} \quad \ldots\ldots\ldots\ldots\ldots\ldots (7),$$

where I is the total cathode current $(I_a + I_s)$.

A hexode operates with a cathode current which is practically constant, the third grid controlling the division of current between second grid (screen) and anode. I and Γ^2 may therefore be taken as constant while m varies at the oscillator frequency. It is then found that the average value of (7) taken over the oscillator cycle is considerably higher than either (4) or (5). That this should be so follows from first principles since one method of reducing partition noise is to increase the ratio of anode to screen currents; (see Chap. 15 Sec. 9.). Anything which reduces this ratio, such as the application of a negative voltage to the third or injector grid, therefore increases partition noise.

From the above arguments it would be expected that a pentode frequency converter would be noisier than a triode and a hexode noisier than a pentode, and this in fact is found to be the case. It is found also that a given valve is noisier as a frequency converter than as a straight amplifier, the mean anode current being the same in both cases; this is mainly due to the lower value of G_c compared with G_m. The table below gives comparative figures for the CV660 valve :-

OPERATION	G_m (MILLIMHO)	G_c (MILLIMHO)	EQUIVALENT NOISE RESISTANCE
Straight Amplifier	9·0	-	720 Ω
Frequency Changer (Triode Connected)	-	4·2	1 kΩ
Frequency Changer (Pentode Connected)	-	3·6	3·5 kΩ

Hexode valves have much higher equivalent noise resistances, the 6SA7, for example, giving a value of 220 kΩ.

The actual noise factors obtainable in frequency changers of the conventional type are not of vital importance as these are always used after a signal frequency amplifier where the signal level, and with it the noise produced in the first signal frequency stage, has been raised to such a value that the noise contribution of the mixer itself is of little account. What is of importance is the number of signal frequency stages needed to do this, which can be decided only if the noise factor of the mixer is known. With careful design a triode frequency changer can be made to have a noise factor of about 11 db at 200 Mc/s; this should be compared with 7·6 db and 5·6 db for the CV66 and CV88 respectively operating as straight amplifiers at the same signal frequency; (see Sec. 14).

26. Noise in Diode Mixers

When discussing the noise present in a diode mixer circuit (see Fig. 702) the mixer and the first IF stage must be considered together. The noise fluctuations in the anode circuit of this stage are then due to the following causes :-

(1) the noise current in the anode circuit of the last RF stage; this includes the inherent noise of this stage together with that generated in the earlier stages and in the aerial, and subsequently amplified.

(2) The thermal noise of the tuned circuit feeding the diode.

(3) The shot noise in the diode itself.

(4) The thermal noise in the IF circuits coupling the diode to the first IF stage.

(5) The shot, partition and transit-time noise of the first IF stage.

It is possible to derive equivalent circuits for the combination of diode mixer and IF stage by methods similar to those adopted for the RF amplifier in Secs. 7 - 14, but the process is more complicated and only a general outline is given here.

The factors which may be adjusted to give the best signal/noise ratio in the IF output are :-

(1) The coupling between the signal frequency circuit and the diode.

(2) The operating conditions of the diode; i.e. bias resistance and local oscillator input.

(3) The coupling between the diode and the IF stage.

At the frequencies at which diodes are used as mixers it is always possible to obtain a gain in the signal frequency stages which is sufficient to over-ride the noise contribution of the mixer, so that, having chosen the operating conditions of the diode, factors (1) and (3) are then adjusted to give maximum signal output. This leads to the matched condition which is discussed in Sec. 21. The overall noise factor of the combined diode and IF stages can then be calculated or measured. It has been found that for any given bias resistor (R_b of Fig. 702) there is an optimum amplitude of the

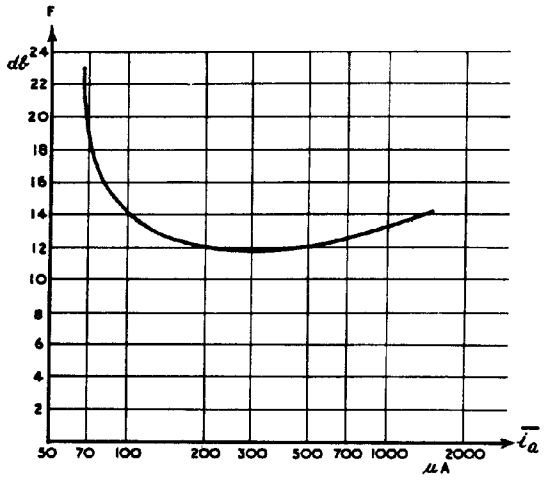

Fig. 712 –
Variation of noise factor with mean diode current.

oscillator input. This is shown in Fig. 712, in which the noise factor for a bias resistor of 5 kΩ is plotted against mean diode current for a CV58 diode followed by a CV1091 IF stage, the signal frequency being 600 Mc/s and the IF 45 Mc/s. The high value of noise factor for low diode currents is due to the high conversion loss for low oscillator inputs. As the oscillator voltage is increased the conversion loss falls but the shot noise of the diode becomes increasingly important as the mean current rises. For high mean currents the increase in shot noise more than counterbalances the decrease in conversion loss.

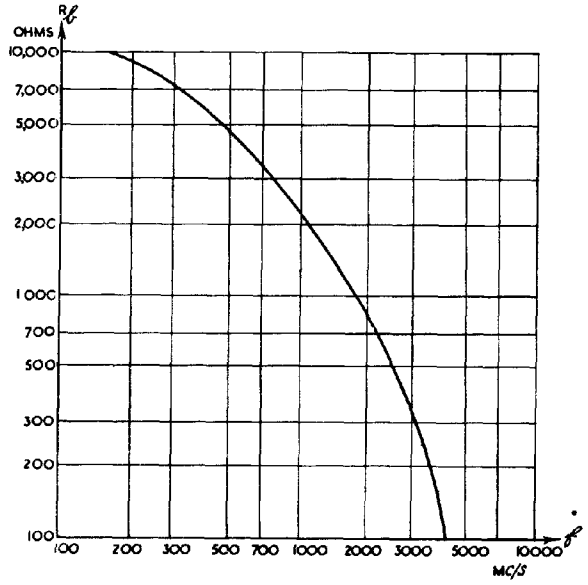

Fig.713 –
Diode mixer: variation of optimum bias resistor with signal frequency.

There is also a best value of bias resistance, which becomes smaller as the frequency increases; (Fig. 713). This reduction in R_b is necessary to offset the increase in the susceptance due to the diode capacitance. When both oscillator input and bias resistance have been adjusted to their optimum values the resultant minimum noise factor varies with frequency in the manner shown in Fig. 714. The CV58 diode has been used at frequencies up to 3,000 Mc/s in applications where its greater freedom from overload damage is more important than the lower noise level of the crystal. For this diode the average noise factor is about 4 db higher than for a crystal, but manufacturing tolerances for the diodes are less rigid, variations between different diodes being greater than in the case of crystals.

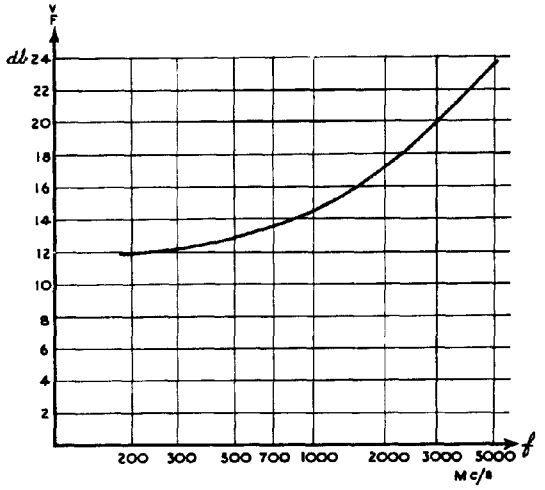

Fig.714 –
Diode mixer: variation of minimum noise factor with signal frequency.

27. Noise in Crystal Mixers

In radar receivers designed for centimetre wavelengths it is not practicable to amplify at the signal frequency so that the mixer must be the first stage in the receiver. Crystals are almost invariably used, and the signal-to-noise ratio of the receiver, and therefore the overall performance of the equipment, depend to a very great extent on

careful design of the crystal and associated circuits for minimum noise.

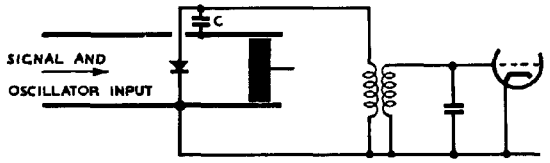

Fig.715.
Basic circuit of crystal mixer and IF stage.

With the diode, two factors have to be adjusted to give the best performance; the bias resistor and the amplitude of the local oscillator input. With the crystal it is found that no bias resistor is needed, the only variable therefore being the local oscillator input which, as in the case of the diode, is most conveniently represented by the mean rectified current which it produces. The crystal is assumed to be matched to the coaxial line or waveguide as described in Sec. 22, so that all the signal power received by the aerial is fed into it. The crystal then acts as a generator at the intermediate frequency, feeding the grid of the first IF stage through a step-up transformer (Fig. 715). It can, in other words, be regarded as replacing the aerial of Sec. 9. The aerial resistance (Fig. 669) must then be replaced by the IF output impedance of the crystal, i.e. by the resistance Ry of the equivalent IF circuit of Fig. 701(b). There will of course be some susceptance in shunt with this due mainly to the RF bypass capacitance C of Figs. 709 and 710 but this will be accommodated by the tuning of the grid circuit of the IF stage.

Owing to conversion loss in the crystal the power developed in the equivalent IF circuit is less than the signal power P_s fed into the crystal. In fact

$$P_s = A \frac{\overline{v_y^2}}{(R_y + R_i)} \quad \ldots\ldots\ldots\ldots\ldots\ldots\ldots\ldots \quad (8)$$

where v_y, R_y and R_i refer to Fig. 701(b) and A is the conversion loss-factor as defined by equation (50) of Sec. 19. R_i is the load on the crystal imposed by the IF input circuit, and includes the dynamic conductance of the tuned circuit, the transit time conductance and the input conductance of the IF valve due to inductance in the cathode lead. The equivalent input circuit for the IF stage is therefore obtained from Fig. 679 by the simple replacement of v_s by v_y, and t^{G}_{r} by t^{G}_{y}, it being remembered that t^{G}_{y} now refers to the transferred IF output conductance of the crystal; (Fig. 716).

When the noise circuit is considered a complication arises owing to the fact that the noise output of the crystal is higher than that corresponding to the thermal noise in a resistor R_y, i.e.

$$\overline{v_n^2} > 4\,k\,T\,B.\,Ry$$

We may therefore write

$$\overline{V_n^2} = x \cdot 4\,k\,T\,B.R_y$$

$$= 4\,k(xT)B.\,R_y$$

$$\ldots\ldots\ldots\ldots\ (9),$$

where x is called the Noise Temperature Ratio of the crystal. Equation (9) shows that an ohmic resistor of value R_y would have to be raised from room temperature T to a higher temperature xT in order to generate the same noise as the crystal. The equivalent noise circuit of Fig. 680 must therefore be modified by increasing the noise current generator representing the aerial noise by the factor x, giving the circuit of Fig. 717. These equivalent circuits have been drawn assuming that the first IF stage is a pentode, but the case of a grounded grid triode in this position may be dealt with in a precisely similar manner.

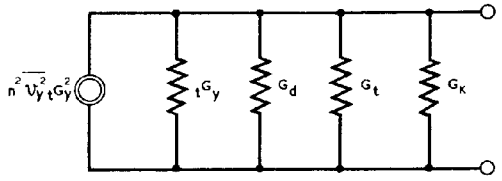

Fig.716.
Equivalent IF input circuit of fig. 715.

Before proceeding to a discussion on the overall noise factor of the crystal and first IF stage it is necessary to examine the factors controlling the noise temperature ratio. The sources of noise are :-

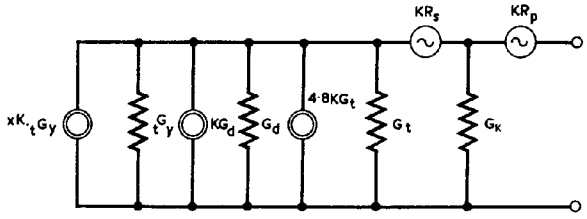

Fig.717.
Equivalent noise input circuit of fig. 715.

(1) noise generated in the aerial system and fed into the crystal with the signal;

(2) noise generated in the crystal itself;

(3) noise produced by the local oscillator and fed into the crystal with the local oscillation.

For the present (3) is neglected. Aerial noise also is unimportant, as, owing to the high conversion loss of crystals, only a fraction of this noise power is developed in the equivalent IF circuit, and measurements have not shown any detectable contribution of aerial noise to the noise temperature ratio.

The problem of the noise generated in the crystal itself is not fully understood. The mechanism of thermal agitation in the barrier layer is much different from that in a homogeneous metal, and further complication arises because the conditions in the crystal are varying rapidly as the working point is moved up and down the non-linear characteristic by the local oscillator input. There appears to be no correlation between the static characteristic of the crystal and the thermal noise generated in it, and when the question is approached practically by taking measurements of conversion loss and noise temperature ratio there is again no correlation, since a low conversion loss

does not imply a low noise temperature ratio.

The IF output conductance, conversion loss and noise temperature ratio all depend on the mean crystal current $\overline{i_0}$. Experimental results for an average crystal operating on about 10,000 Mc/s are shown in Figs. 718 and 719.

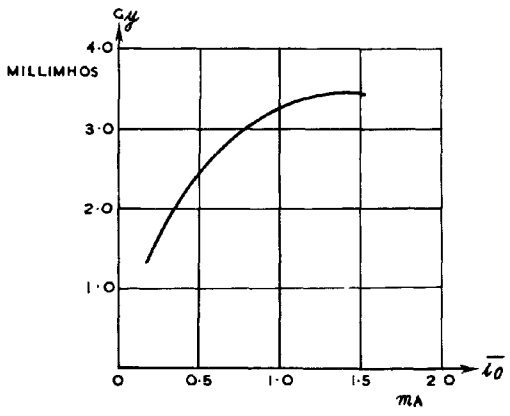

Fig.718.
Variation of IF output conductance of crystal with mean crystal current.

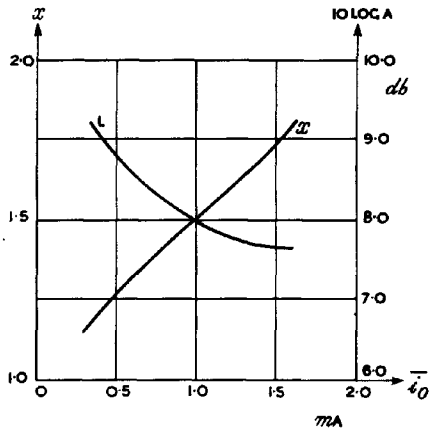

Fig.719.
Variation of noise temperature ratio and conversion loss with mean crystal current.

28. Local Oscillator Noise

The local oscillator used in a radar receiver operating on centimetre wavelengths is usually a klystron, and this type of valve produces, in addition to the desired oscillation of frequency f_0, random noise which is most intense at frequencies close to f_0. The amplitude spectrum of the output of the klystron is indicated in Fig. 720. The amplitude of the noise relative to the desired oscillation is, of course, very much smaller than is shown in the figure. To understand how this noise is produced, consider the double rhumbatron klystron shown diagrammatically in Fig. 721. The local oscillator (Sutton Tube) is of the reflector, or single-rhumbatron type, but the mechanism of noise production is similar and the explanation is more easily followed with the double-rhumbatron type. The operation of both double-rhumbatron and reflector type klystrons is explained in Chap. 8 Secs. 21-23.

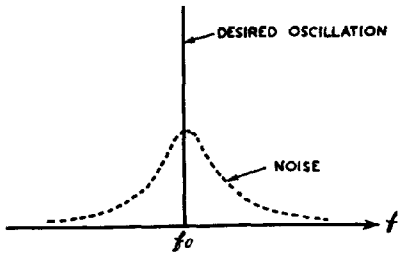

Fig.720.
Amplitude spectrum of output of klystron local oscillator.

The mechanism of noise production is as follows. The electron beam entering the buncher at A is not uniform but is intensity modulated in a random manner due to the shot noise fluctuations of the emission from the cathode. The buncher then

acts as a catcher for the shot noise fluctuations and noise current will thus be induced in it in a manner similar to that in which induced grid noise currents are set up in a negative-grid triode. These noise currents are relatively large since the electrons are travelling at high speed, and it is due to them that klystrons are too noisy to be used with advantage as amplifiers for small signal voltages.

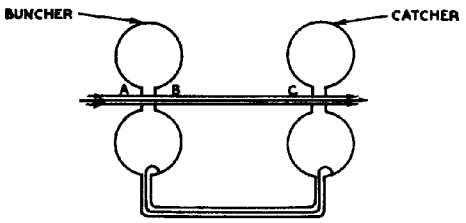

Fig. 721 – Double-rhumbatron type of klystron.

The noise voltages generated in the buncher modulate the velocity of the main electron stream and thus appear in an amplified form in the catcher. Further amplification is provided by the regenerative coupling between the rhumbatrons. The shot noise fluctuations have an amplitude spectrum which is uniform over all frequencies but the rhumbatrons are frequency-selective and respond only to frequencies near resonance, i.e. close to f_o. The resultant noise voltages are therefore largest for frequencies close to f_o, the amplitude falling off rapidly as the frequency separation from f_o increases. The general nature of the amplitude spectrum is thus as shown in Fig. 720. As would be expected, the frequency spread of the noise voltages depends on the selectivity of the rhumbatrons, high-Q rhumbatrons giving a small spread and vice versa.

The output circuit of the mixer is tuned to the intermediate frequency and therefore it is necessary to consider only those local oscillator noise components, which, after passing through the crystal, produce an output lying within the pass-band of the IF amplifier. If f_o is the frequency of the local oscillator, f_i the intermediate frequency and B the band width of the IF amplifier, then the effective local oscillator noise components are those lying in the two frequency ranges.

$$(1)\quad f_o - f_i \pm \frac{1}{2} B$$

and

$$(2)\quad f_o + f_i \pm \frac{1}{2} B.$$

It is these which give IF outputs by first order mixing with the local oscillation. The noise produced by mixing between the individual noise components themselves and between noise components and signal is negligible. The relevant frequency bands are shown in Fig. 722.

From what has been said of the fundamental cause of klystron noise it follows that it is essentially a selectivity problem and any factors leading to a low degree of selectivity increase the contribution of local oscillator noise to the noise temperature ratio. The two most important are :-

(1) a low-Q rhumbatron

(2) a low value of f_i/f_o.

It is therefore not surprising that local oscillator noise is very small at 3,000 Mc/s and becomes increasingly important as the operating frequency is raised. At 10,000 Mc/s, with an IF of 45 Mc/s, the CV87

and CV129 klystrons produce a very small amount of oscillator noise, but with the CV720 about half the noise temperature ratio of the crystal is due to the local oscillator, average values of x being 1·5 for the CV129 and 3·0 for the CV720. The higher value for the CV720 is due to the smaller dimensions of its cavity, which thus has a lower Q.

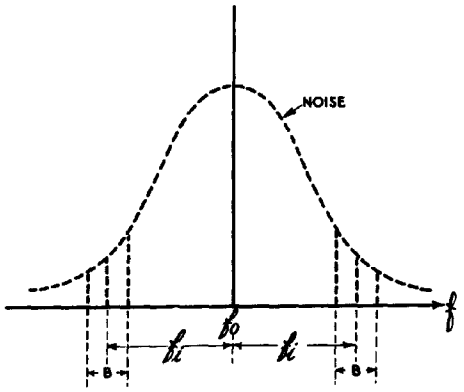

Fig.722.
Amplitude spectrum of output of local oscillator showing noise components producing IF noise in mixer output.

Another point of interest with the CV720 arises from its use in AFC circuits (Chap. 8 Secs. 49-53) where a certain amount of control over the oscillation frequency is obtained by variation of the reflector voltage. Measurements show that if too great a frequency variation is attempted by this means the noise temperature ratio rises sharply, causing a serious deterioration in the signal/noise ratio of the equipment. Typical results are shown in Fig. 723.

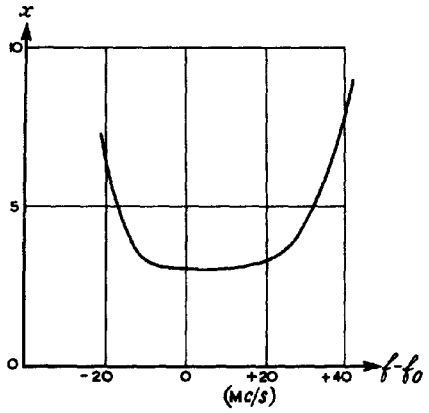

Fig.723.
Dependence of noise temperature ratio on change of frequency produced by variation of reflector volts (90-volt mode of CV 720).

At a frequency of 24,000 Mc/s most of the noise output of the crystal is due to the local oscillator, noise temperature ratios up to 10 being common. The comparison between results at this frequency and at 10,000 Mc/s is shown in Fig. 724, which also shows the improvement in noise temperature ratio consequent on the use of a high IF with a corresponding increase of f_i/f_o. The 24,000 Mc/s curves of Fig. 724 are drawn for two different values of crystal current, the higher value of crystal current giving the higher noise temperature ratio. This is to be expected, since increasing the local oscillator input to the crystal also increases the noise input.

With a general tendency towards increasing operating frequencies attention has been focused on methods of reducing the local oscillator noise. Amongst the methods suggested are :-

(1) the use of a high-Q rhumbatron cavity in the local oscillator.

(2) the use of a high value of IF.

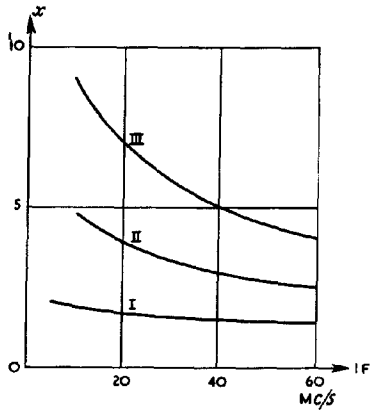

Fig.724 – Dependence of contribution of local oscillator noise on intermediate frequency,
Curve I: 10,000 Mc/s. Mean crystal current = 0.5 mA
Curve II: 24,000 Mc/s. Mean crystal current = 0.25mA
Curve III: 24,000 Mc/s. Mean crystal current = 0.5 mA

(3) filtering the local oscillator output by means of a high-Q cavity between oscillator and mixer.

(4) eliminating one of the noise-frequency bands of Fig.722. One of these contains the signal and cannot be removed, but the "second channel" can be cut out by suitably positioning the TR cell; (see Sec. 34).

(5) the use of two mixers in a balanced circuit. The signal outputs are made to add while the noise outputs due to the local oscillator are in antiphase and are therefore cancelled.

29. The Overall Noise Factor of Crystal Mixer and IF Amplifier

As described in Sec. 27, in centimetre receivers it is assumed that the feeder is matched to the crystal so that the aerial resistance R_r of Sec. 8 is replaced by the mixer output resistance R_y of Sec. 19; (see equation (50) of that section and Fig. 701(b)). For an ideal centimetric receiver we assume that all the signal power is supplied to the IF circuit, i.e. that there is no conversion loss, and that the only noise present is that due to thermal noise in R_y.

The equivalent signal and noise circuits for the actual receiver are given by Figs. 716 and 717.

From Fig. 716 the mean square IF voltage at the first grid is given as :-

$$\frac{}{s^2} = \frac{n^2 \overline{v_y^2}\ t G_y^2}{G^2} \quad \text{where } G = t G_y + G_d + G_t + G_K \ldots\ldots (10)$$

From Fig. 717 the mean square noise voltage at the first grid is given as :-

$$\overline{n^{v2}} = \frac{K(x.\ {}_tG_y + G_d + 4{\cdot}8\ G_t)}{G^2} + K\,R_s\,\frac{(t^{G_y} + G_d + G_t)^2}{G^2} + K\,R_p$$

..... (11).

Hence, for the actual receiver,

$$\frac{n^P}{s^P} = \frac{\overline{n^{v2}}}{\overline{s^{v2}}} = \frac{K\,(x.t^{G_y} + G_d + 4{\cdot}8\ G_t) + K\,R_s\,(t^{G_y} + G_d + G_t)^2 + K\,R_p\,G^2}{n^2\ \overline{v_y^2}\ tG_y^2}$$

..... (12).

For the ideal receiver described above, two modifications to the equivalent circuits are necessary.

(i) Fig. 716. Since there is no conversion loss the mean square signal voltage must be increased by a factor A.

(ii) Fig. 717. Since the only noise present is thermal noise in R_y (Fig. 701(b)) the noise generator $x.{}_tG_y$ must be replaced by ${}_tG_y$, and the other noise generators must be suppressed.

These modifications are illustrated in the equivalent circuit of Fig. 725. Hence, for the ideal receiver, after making these alterations to equation (12) we obtain :-

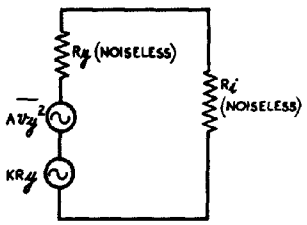

Fig.725 - Equivalent IF input circuit of ideal receiver with crystal mixer.

$$\frac{n^P}{s^P} = \frac{\overline{n^{v2}}}{\overline{s^{v2}}} = \frac{K\ {}_tG_y}{A\ n^2\ \overline{v_y^2}\ .\ tG_y^2}\ ,\ \ldots\ldots\ldots\ldots\ (13).$$

By definition, the noise factor F is the quotient of (12) and (13), viz:-

$$F = A\left\{x + \frac{G_d}{tG_y} + \frac{4{\cdot}8\ G_t}{tG_y} + \frac{(tG_y + G_d + G_t)^2.\ R_s}{tG_y} + \frac{G^2}{tG_y}.\ R_p\right\}$$

..... (14).

If the noise factor F_i due to the IF amplifier alone is required, it can be obtained directly from equation (24) of Sec. 12 on making the appropriate substitutions. The result is :-

$$F_i = 1 + \frac{G_d}{{}_tG_y} + \frac{4{\cdot}8\ G_t}{{}_tG_y} + \frac{(tG_y + G_d + G_t)^2 \cdot R_s}{{}_tG_y} + \frac{G^2}{{}_tG_y} \cdot R_p$$

..... (15).

A comparison of equations (14) and (15) shows that

$$F = A\left\{F_i + x - 1\right\} \quad \text{..... (16).}$$

This result is a particular case of a general theorem for the overall noise factor of several amplifiers or other networks in cascade. If F_1, F_2, ------, F_n are the noise factors of the individual networks; and M_1, M_2, --------, M_n the power amplification ratios, the overall noise factor is given by

$$F = F_1 + \frac{F_2 - 1}{M_1} + \frac{F_3 - 1}{M_1 M_2} + \text{.....} + \frac{F_n - 1}{M_1 M_2 \ldots M_{n-1}} \text{.....} \quad (17).$$

In the particular case of equation (16), F_1, the noise factor for the crystal itself, is Ax, and $M_1 = \frac{1}{A}$, while $F_2 = F_i$. With these substitutions (16) is the same as (17) for n = 2.

When (15) is differentiated to find the optimum transferred crystal IF output conductance ${}_tG_y$, the value obtained depends on neither A nor x, for A is merely a multiplying constant and x disappears on differentiation. The minimum overall noise factor F is thus obtained by designing the coupling transformer between the mixer and the first IF stage for a minimum value of F_i.

Since the IF output conductance of the crystal is a function of the mean crystal current (see Fig. 718) it follows that the optimum turns ratio will also depend on the mean crystal current. Once the best operating conditions have been settled it is therefore essential to maintain the correct value of mean crystal current when the receiver is in operation. Failure to do so may cause deterioration in performance.

Values of A and x for an average 10,000 Mc/s crystal are given in Fig. 719. If these values are substituted in equation (16) the results of Fig. 726 are obtained. Two alternative values of F_i, 3 db and 5 db, have been used in calculating these curves. The minimum is due to exactly the same cause as the minimum in the corresponding curve

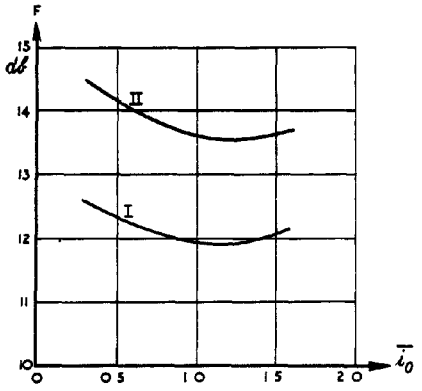

Fig.726.
Overall minimum noise factor of IF amplifier and crystal of fig. 720.
$F = A(F_i + x - 1)$
Curve I: F_i = 2(3db)
Curve II: F_i = 3·16(5db)

for the diode (Fig. 712): for small mean crystal currents the conversion loss is high while for large mean currents the crystal noise increases in greater proportion than the decrease in conversion loss.

RADAR RECEIVERS

30. General

In a superheterodyne receiver amplification is obtained in three ways :-

(1) in the signal frequency stages;

(2) in the IF stages after frequency conversion;

(3) in the video stages after detection.

The amplitude of the output from the video amplifier depends on the type of display used. This amplifier must have a band-width sufficient for reasonable pulse reproduction and a gain high enough to give the required output with the given input from the detector.

The detector output, although it is not critical, must lie within well defined limits. A diode is normally the most usual form of detector and this must have a small resistance load if the pulse-shape is to be preserved. Under these conditions the detection efficiency is lower than that common in communication receivers, and the non-linearity of the rectification characteristic at low input levels is more pronounced. With a typical diode (e.g. CV1092) the peak output should not fall much below 1 volt if sensitivity is not to suffer. On the other hand it is not possible to obtain large outputs from the diode without producing overloading in the IF stage preceding it. With the bandwidths commonly used the anode loads of the IF stages must be low (see Chap. 7) and unless the complication of a larger last IF valve is indulged in the detector output begins to be non-linear beyond about 10 volts (peak). The useful output from the detector is thus about 5 volts (peak) and the video amplifier is designed to give the requisite output to the display for this value of input.

It is then necessary to decide how much of the pre-detection gain should be provided by the signal frequency amplifier and how much by the IF amplifier. As a general rule the lower the frequency the easier it is to obtain amplification and maintain stability; moreover, the tuning of the IF amplifier is preset, whereas the signal frequency stages must have provision for varying the tuning to follow alterations in the operating frequency. It is thus desirable to introduce the mixer at the earliest possible place in the amplifier chain. The only reason for using signal frequency amplification at all in radar design is the fact that the noise factor of mixers is in general higher than that of signal amplifiers. If it were possible to produce a mixer with a noise factor as low as that of the signal amplifier the latter could be dispensed with, producing a considerable simplification of the receiver.

31. The Overall Noise Factor of a Receiver

The overall noise factor of a crystal mixer followed by an IF amplifier is dealt with in Sec. 29. The diode and IF amplifier combination also is studied in Sec. 26 and the general problem of RF amplifier noise in Secs. 7-14. In these sections it is assumed that the amplifier stages are linear and the problem is approached by a comparison of the signal and noise powers present at different points. Since signal

and noise are statistically independent sources their mean square values are directly additive, the total power then being the sum of the respective signal and noise powers. It is thus possible to define the overall noise factor of the receiver by comparing the signal and noise powers at the output of the IF amplifier with their values at the aerial or crystal; for although a fundamentally non-linear response is an essential feature of a mixer, nevertheless the mixer equivalent circuits have been shown to be representable to a first approximation by linear circuit elements; (Secs. 15 - 29). Such a simplification is not possible in the case of the video detector, where we are concerned primarily with the envelopes of the signal and noise voltages, and a power concept is not directly applicable. It is therefore common practice to quote the overall noise figure of the receiver as referring to the output of the IF amplifier. From this the minimum received signal power for a "just detectable" signal can be estimated, it being assumed that "just detectable" means equality of signal and noise power at the IF output. A further complication is introduced by the display since it requires a much larger signal to noise ratio at the detector input to produce a clearly defined echo on a PPI than on an A-display. The standard of equal signal and noise powers at the IF output will tend to underestimate the receiver capabilities on a type A-display and to overestimate them if a PPI is used.

32. The Number of Signal Frequency Stages

When amplifier stages are operated in cascade it is possible to deduce the overall noise factor if the noise factors of the individual stages are known. Fig. 727 shows a block diagram of a receiver with the two signal frequency stages preceding the mixer, the latter and the IF amplifier being regarded as one unit in accordance with Secs. 20-29. The overall noise factor up to the IF output is then :-

$$F = F_1 + \frac{F_2 - 1}{M_1} + \frac{F_3 - 1}{M_1 M_2} \quad \ldots\ldots(1)$$

(see Sec. 29).

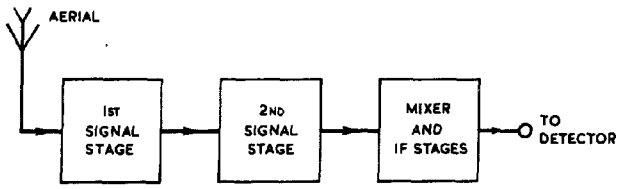

Fig. 727- Block diagram of receiver with two signal frequency stages.

where F_1 and M_1 are the noise factor and power amplification respectively of the first signal frequency stage, F_2 and M_2 refer similarly to the second signal frequency stage and F_3 is the overall noise factor of the mixer and IF stages.

As the first numerical example consider a receiver operating at 30 Mc/s (about the lowest radar frequency). Let F_1 and F_2 be 2 (i.e. 3db) while F_3 is 16, these being reasonable values for CV1136 valves followed by a diode mixer (see Figs. 687 and 714). The power amplification of each signal frequency stage is taken to be 10 so that the overall noise figure from equation (1) is

$$F = 2 + \frac{1}{10} + \frac{15}{100} = 2{\cdot}25 \quad \ldots\ldots\ldots\ldots\ldots\ldots\ldots\ldots (2).$$

The number of signal frequency stages has been chosen arbitrarily and it is instructive to examine how the noise factor changes as the number of these stages is altered. With no signal stage the noise factor would, of course, be that of the mixer and IF stages, i.e., 16. With only one signal stage the mixer is now the second stage so that the last term in (J) is omitted and F_2 replaced by F_3 giving

$$F = 2 + \frac{15}{10} = 3{\cdot}5 \quad \ldots\ldots\ldots\ldots\ldots\ldots\ldots\ldots \quad (3).$$

With three signal stages,

$$F = 2 + \frac{1}{10} + \frac{1}{100} + \frac{15}{1000} = 2{\cdot}125 \quad \ldots\ldots\ldots\ldots \quad (4).$$

These figures are tabulated below : (Table I)

Number of signal frequency stages	Noise factor F Ratio	db.
0	16	12.0
1	3.5	5.4
2	2.255	3.5
3	2.125	3.3

Two points should be noted: (i) the large improvement (6·6 db) produced by the use of only one signal frequency stage (ii) the very small improvement (0·2 db) when the number of such stages is increased from two to three.

As the second numerical example a signal frequency of 200 Mc/s is chosen, again with CV1136 signal amplifiers preceding the diode frequency converter. From Fig. 687 the noise factor of each signal frequency stage is 11·2 (10·5 db) whereas the noise factor of the diode has not increased appreciably. Assuming that by suitable circuit construction the power amplification can be maintained at its original value of 10, the variation of overall noise factor with the number of signal frequency stages is given in table II.

Table II

Number of signal frequency stages	Noise factor F Ratio	db
0	16	12·0
1	12·7	11·0
2	12·4	10·9
3	12·3	10·9

The improvement in noise factor resulting from the use of one signal frequency stage is now only 1db and the further improvement when more stages are added is negligible. It is clear that the use of CV1136 valves at this frequency is of doubtful benefit, the additional complications of such stages not being balanced by any substantial increase in signal/noise ratio. This is , of course, due to the high noise factor of the CV1136 itself and it must be replaced by a valve of lower noise factor if a substantial improvement is sought. The CV66 has a noise factor of 7·6. db at 200 Mc/s (Fig. 687) which gives overall noise factors of 8·6 db and 8·0 db for one and two stages respectively.

At higher frequencies, say 600 Mc/s, valves such as the CV88 must be used (See Sec. 13). The noise factor of this valve is 10db at 600 Mc/s while that of the diode has risen to 13·4 db (Fig. 714). One signal frequency stage will then give an overall noise factor of 10·8 db

which is reduced by only 0·3 db if a second stage is added. It is therefore sufficient to use one stage preceding the mixer.

33. Receiver for Metre and Decimetre Wavelengths.

The technique employed in the design of radar receivers causes them to fall into two general classes according to the operating frequency; (i) up to 600 Mc/s (ii) above 3000 Mc/s. The upper limit of range (i) approaches the limit of usefulness of valve amplifiers and conventional type oscillators, while the use of waveguides and cavity resonators is not practicable much below the lower limit of range (ii) as they would have to be large and cumbersome. There is a further natural subdivision at about 200 Mc/s, for this represents not only the upper limit of the useful range of the pentode but is also the frequency at which conventional lumped circuits must give way to coaxial lines in which inductance and capacitance are distributed. While the use of coaxial line circuits below this frequency is theoretically advantageous, their use is again precluded on the grounds of excessive bulkiness. Some details of receivers for frequencies up to 600 Mc/s are tabulated below (Table III). These illustrate the points which have been studied in the preceding paragraphs.

TABLE III

Receiver	Operating frequency Mc/s	Number of signal freq. stages	Valve type used in signal amp.	Type of tuned circuit	Valve type used in mixer
A	20-60	3	pentode	lumped	hexode
B	55-84	5	pentode	lumped	diode
C	176	2	pentode	lumped	pentode
D	212	2	triode	lumped	pentode
E	212	2	pentode	coaxial	triode
F	600	1	triode	coaxial	diode

34. Receivers for Centimetre Wavelengths

As signal frequency amplification is not practicable at frequencies of 3000 Mc/s nd upwards, the first stage in a receiver operating at such frequencies is of necessity the mixer. A possible arrangement of the signal frequency unit of a receiver operating at about 10,000 Mc/s is shown in Fig. 728. The mixer must be located in the same box as the magnetron if a long and cumbersome waveguide connection between the TR circuits and the mixer is to be avoided. The IF output impedance of the mixer is of the order of 300 ohms (see Sec. 22) and this should be the impedance presented at the connection to the tuned circuit at the grid of the first IF stage. It is therefore not possible to use a long length of cable to connect the mixer to this stage, for the characteristic impedance of such a cable is never far different from 80 ohms and with such a mismatch at the mixer end a considerable susceptance would be present at the connection to

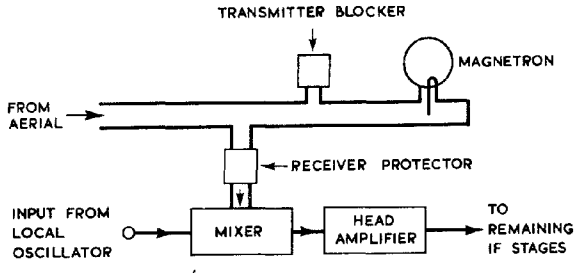

Fig.728.
Block layout of signal frequency unit of 10,000 Mc/s receiver.

the IF tuned circuit. It is also impracticable to use a step-down transformer at the mixer end of the cable since the extra losses present in such a transformer would be an additonal source of noise. It is therefore standard practice to split the IF amplifier into two parts, the first stage or stages being situated close to the mixer and connected to it by a few inches only of screened cable. These stages are called the Pre-Amplifier or Head Amplifier (see Fig. 728). The remaining IF stages are located in the main amplifier unit. Matching transformers or other devices are used, normally at both ends of the cable connecting the head amplifier to the receiver unit, the additional noise introduced by placing them at this point in the amplifier chain being negligible.

The first stage in the head amplifier is critical from the point of view of signal/noise ratio (see Sec. 9). Earlier receivers used a pentode in this stage, but more recent developments, particularly the production of crystals with lower noise temperatures, have enabled a substantial improvement to be obtained by the use of grounded-grid or neutralised triodes in head amplifiers.

35. The IF Amplifier

The gain of this amplifier should be sufficient to give full output from the detector on inherent noise alone, and this gain is easily calculated.

Consider the case of an IF amplifier with a pentode first stage following a crystal mixer; the mean square noise voltage $\overline{n^{v2}}$ at the grid of this valve is given by equation (11) of Sec. 29.

$$\overline{n^{v2}} = K\,\frac{(x\,.\,t^{G_y} + G_d + 4{\cdot}8\,G_t)}{G^2} + KR_s\,\frac{(t^{G_r} + G_d + G_t)^2}{G^2} + KR_p \qquad \ldots\ldots\ldots\ldots\ldots\ldots\ldots\ldots (5),$$

where x is the noise temperature ratio and t^{G_y} the transferred IF output conductance of the crystal, the remaining quantities being as defined in Secs. 10-12. Substituting the appropriate values for the CV1091 from Sec. 12 for an IF of 45 Mc/s and a crystal noise temperature ratio of 1·5, the equivalent RMS noise voltage at the grid is found to be 15·6 microvolts. A voltage amplification of the order of 10^6 will thus be needed to give full detector output. It is therefore usual to find about 5 stages in the IF amplifier proper, which, together with the two stages in the head amplifier, give a total of 7 IF stages.

The above argument applies only to receivers for centimetre wavelengths. At lower frequencies part of the required amplification is obtained at the signal frequency and the number of IF stages may then be reduced to 4 or 5.

The amplifier itself calls for little comment but it should be remembered that the necessity for providing an overall voltage amplification of about 10^6 at a frequency as high as 45 Mc/s involves very careful screening and the use of elaborate decoupling and filtering circuits in the supply leads. The required bandwidth is obtained either by staggered tuning or coupled tuned circuits or by a combination of the two (see Chap. 7).

36. Manual gain control

The gain of the receiver is varied by changing the gain of the IF amplifier by one of two usual methods:

(1) The voltage applied to the screens is kept constant and a variable negative voltage applied to the control grids.

(2) The control grids are kept at fixed potentials of about -1·5 volts and the screen voltages are varied.

The latter method is to be preferred since it is found that the change in input impedance of a RF amplifier valve is less marked when the mutual conductance is altered by varying the screen voltage than when the alteration is produced by a variation of the control grid potential. Since the combined screen currents of the controlled valves may exceed 10 mA the screens may be fed from the cathode of a Gain Control Valve, which is simply a cathode follower, the grid potential of which is determined by a potentiometer across the HT supply. By this means the use of a heavy duty potentiometer to supply the screens is avoided.

When strong signals are being received the gain control must be set near the position for minimum gain, and if the last IF stage were controlled it would be difficult to secure adequate output without overloading at the input. This stage is therefore operated with fixed electrode potentials. Gain control is not normally used on signal frequency amplifiers or IF head amplifiers as the operating conditions of these must be kept fixed if the optimum noise factor is to be maintained.

37. A.G.C.

Automatic gain control (AGC) is applied to communication receivers for the purpose of stabilising the carrier amplitude at the detector. This is accomplished by the standard method of rectifying the output from the last IF stage, filtering out the modulation frequency components and applying the resultant steady voltage (which must be of negative polarity) to the control grids of some of the signal frequency and IF valves. This method is suitable only when a continuous carrier is being radiated and cannot be applied to a radar receiver where the received signal consists of very short pulses of RF energy.

In radar reception it is the pulse amplitude at the display that must be stabilised and it is also essential to use some method of pulse selection so that AGC is operative only with respect to one particular echo. Fig. 729 shows a typical A-type display with the transmitter pulse (A) and five target echoes (B to F). One method of determining range is to set the echo required, for example D, with its leading edge on the vertical cross-wire, the range being read from the setting of the X-shift potentiometer. To ensure consistent range measurement the amplitude of D on the screen must be stabilised by AGC, the resultant amplitude being completely independent of the number and amplitudes of other target echoes which may be present.

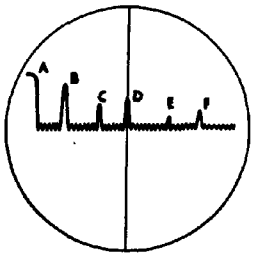

Fig.729. A-type display showing transmitter pulse (A) and five target echoes (B to F).

The AGC voltage is obtained from a peak rectifier operated from the output of the video amplifier, a gating circuit being used to ensure that only the required echo is passed to the AGC rectifier. The circuit of a typical AGC system is shown in block diagram form in

Fig. 730; the gate valve circuit is given in Fig. 731 and the relevant waveforms in Fig. 732. There are two video stages between the detector and the cathode-ray tube, a third stage (VIDEO 3 of Fig. 730) being used to feed the AGC system. The output from the detector is of positive polarity so that positive pulses are fed from the VIDEO 3 stage to the gate circuit. The output from the time-base generator is fed to the gate pulse generator which produces a short positive pulse as the spot passes across the centre line of the tube, the duration of this pulse being not much greater than that of a received echo. The pentode gate valve (Valve 2 Fig. 731) has its cathode held positive by virtue of the current through R_1 and R_2 and its current is normally cut off at both control and suppressor grids. The transmitter break-through pulse A and the received echoes B, C, E and F carry the control grid above cut-off, but no voltage is developed at the anode as the anode current is cut off at the suppressor grid. During the gating pulse the suppressor is at cathode potential and the pulse D applied to the control grid produces a negative-going pulse at the anode which is passed to the AGC peak rectifier. If no target echo is received during the gating pulse the sensitivity of the receiver rises until the inherent noise passes through the gate valve and operates the AGC rectifier, thus stabilising the height of the "grass" on the tube. Valve 1 of Fig. 731 is a clamping diode, preventing the suppressor from going positive with respect to the cathode (Chap. 12).

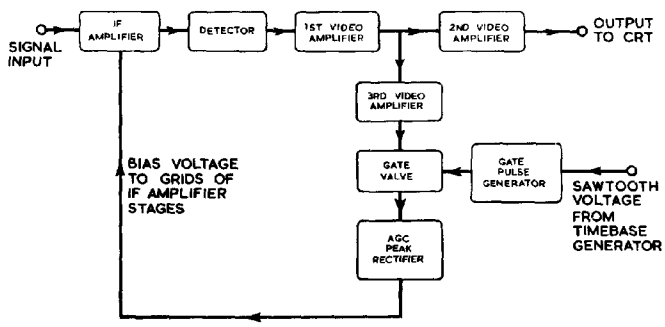

Fig.730_ Block diagram of AGC system.

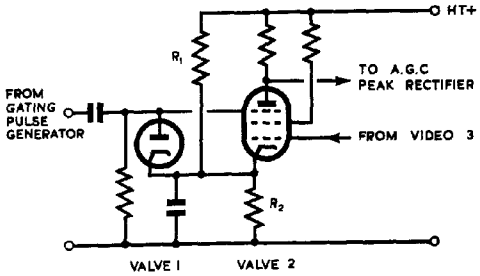

Fig.731_ Circuit of gate valve.

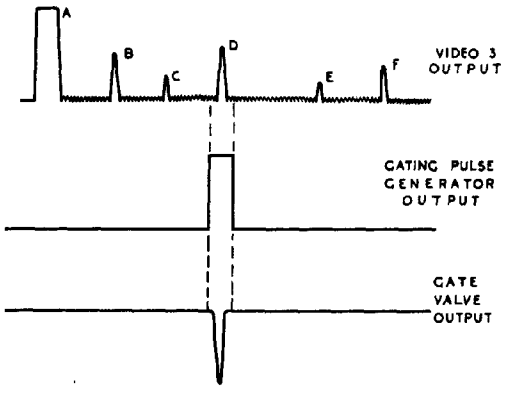

Fig.732_ Waveforms of gating circuit.

38. Paralysis

The radar receiver is highly sensitive and is usually placed close to the powerful transmitter; in fact, with common T/R working the two are connected to the same aerial. A very large signal is thus received during the transmitter pulse and may result in a loss of receiver sensitivity for some little time after this pulse has ceased, the reception of echoes from nearby targets thus being rendered difficult or impossible. This temporary paralysis may occur in either grid or cathode circuits or in both, but it is convenient to consider the two cases separately.

(i) Grid paralysis

A positive voltage applied to the grid of any valve causes grid current to flow, and if the coupling is suitable, bias may be developed. In Fig. 733 the large voltage produced across the anode load of valve 1 during the transmitter pulse causes the grid of valve 2 to draw grid current, with the result that this grid is left negatively charged at the end of the transmitter pulse. This negative charge leaks away at a rate determined by the time constant $C_c R_g$ of the coupling circuit. Valve 2 is thus biased back at the beginning of the time-base sweep, or the current may even be cut off, so that the receiver sensitivity is reduced below its normal value and may not have recovered completely before the spot on the cathode ray tube has reached the end of its travel. The circuit of Fig. 734 is free from this defect, for although the condenser C_c is charged during the transmitter pulse the resistance of the tuned circuit to direct currents is so low that no appreciable bias voltage is developed across it. The charging and discharging of C_c now produce changes in the mean anode voltage of valve 1, which do not affect the receiver sensitivity to any marked extent.

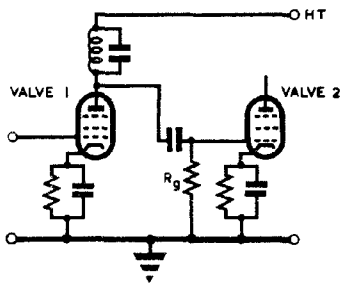

Fig. 733 – Coupling circuit producing grid paralysis.

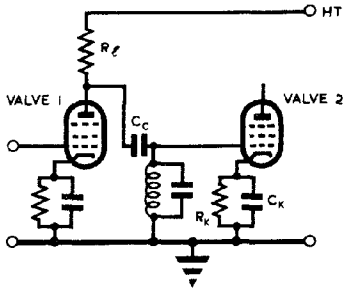

Fig. 734 – Coupling circuit free from grid paralysis.

The circuits of Figs. 733 and 734 show automatic bias for the amplifier stages. When fixed bias is used, in order to give manual gain control by variation of the screen voltage, as in Fig. 735, paralysis may be produced by the charging of the bias decoupling condenser C_b which must discharge through the decoupling resistor R_b before the grid can return to its normal potential. In this case paralysis may be

cured by connecting a large condenser, say 10 microfarads, across C_b. The resultant capacitance is not charged to any appreciable extent by the flow of grid current during the transmitter pulse, and while the mean rectified current must flow through R_b and thus produce a voltage drop across it, this is very small. C_b, which for 45 Mc/s. has a value of about 0·001 microfarad, must be retained, as electrolytic condensers are not effective for RF by-passing.

(ii) Cathode paralysis

During the transmitter pulse the grid receives a very large signal and rectification takes place in the anode circuit as well as the grid circuit, the mean cathode current rising well above its normal value. The cathode by-pass condenser, C_K of Fig. 734 then charges, and at the end of the transmitter pulse the cathode may be sufficiently positive for the valve current to be cut off. Even if this does not happen the sensitivity is reduced until the cathode has returned to its normal working potential.

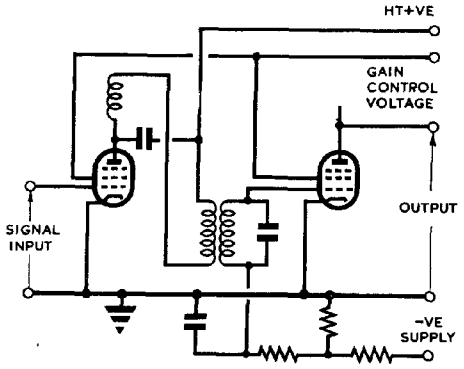

Fig.735 – Coupling circuit for fixed bias.

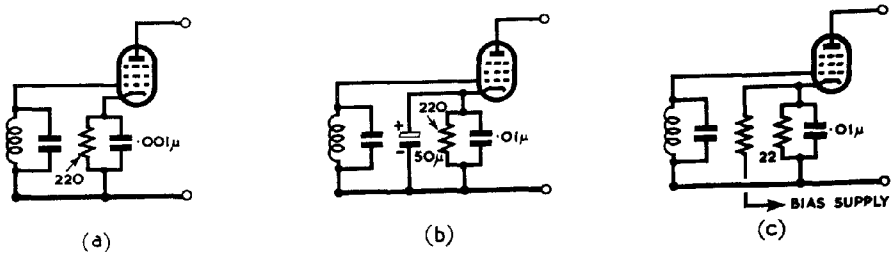

Fig.736 – Circuits for eliminating cathode paralysis

Cathode paralysis may be dealt with in one of three ways :-

(1) The time-constant of the cathode circuit may be made so short that at the end of the transmitter pulse the cathode returns very quickly to its normal potential. In Fig. 736 (a), which is suitable for an IF stage operating at 45 Mc/s., the by-pass condenser of 0·001 μF is sufficient for thorough decoupling of the cathode at this frequency, while the time constant $C_K R_K$ is only 0·22 microsecond.

(2) If the IF is considerably lower the by-pass condenser must be increased with a corresponding increase in the

time constant, which may then become too long. In this case the RF by-pass condenser is shunted by a large electrolytic condenser (Fig. 736(b)), which prevents the cathode potential from rising to any appreciable extent during the transmitter pulse.

(3) As an alternative to (2), the time constant may be kept low by decreasing the bias resistor, the additional current required to maintain the required bias being obtained from a separate bias supply (Fig. 736(c)). This system is rather wasteful in current, since the bias supply must deliver a considerably greater current than the normal cathode current of the valve (nine times as much in the case of the circuit of Fig. 736 (c)).

39. Receiver Suppression

If the large signal produced by the transmitter pulse can be prevented from reaching the receiver paralysis can be avoided. At first sight, the simplest method is to short-circuit the input during the transmitter pulse but this presents some difficulties. A mechanical relay is not sufficiently rapid, and all electronic switches have appreciable voltage developed across them by a large signal. With common T/R working such electronic switching is, of course, adopted, but the breakthrough from the transmitter pulse is still able to cause paralysis.

The most satisfactory method of overcoming these difficulties is to "suppress" the receiver during the transmitter pulse. In many radar equipments a 20 microsecond Priming pulse is used, the trailing edge of which coincides with the start of the transmitter pulse (Fig. 737). This priming pulse is inverted to give negative polarity, passed through a suitable delay circuit and is then applied as a suppression pulse to the suppressor grids of some of the signal frequency or IF stages of the receiver, thus rendering the latter inoperative during the transmitter pulse.

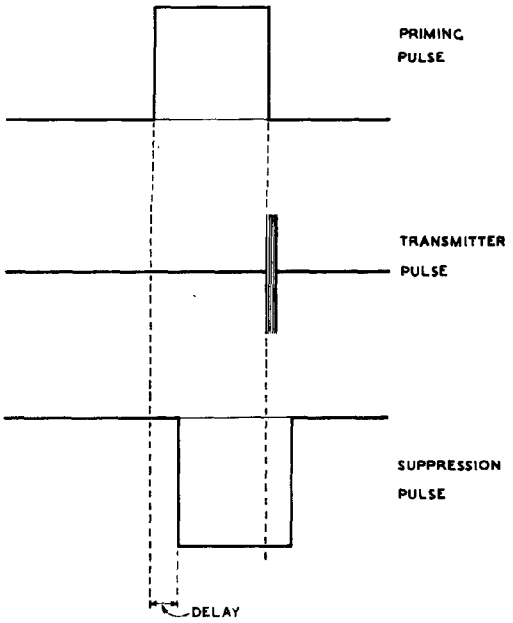

Fig.737. Waveforms of simple suppression circuit.

40. Anti-Clutter Gain Control (Swept Gain)

The signals received from nearby objects are very much stronger than those received from objects which are more distant. If the gain of the receiver is increased so as to receive the latter, the former may be strong enough to saturate the receiver and may even produce paralysis (Fig. 738). It is therefore desirable to have some means of varying the gain automatically as the spot moves across the screen, the

gain being low at the beginning of the trace and reaching maximum as the spot moves to the end of its travel. Instead of the simple square-pulse suppression waveform of Fig. 737 a more complicated waveform such as that of Fig.739 is applied to the suppressor grids to give automatic variation of gain with range. After the transmitter pulse has ceased the voltage on the suppressors does not immediately rise to zero as in Fig. 737 but rises instead to a value just above suppressor cut-off (A of Fig. 739). During the time-base sweep the voltage rises exponentially to zero, the gain thus increasing along the time-base sweep. There are three variables which have to be adjusted for best results :-

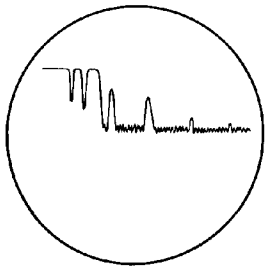

Fig.738 - A-type display showing saturation produced by echoes from objects at close range.

(1) the suppressor voltage at A,

(2) the time-constant of the exponential rise AB, and

(3) the delay time.

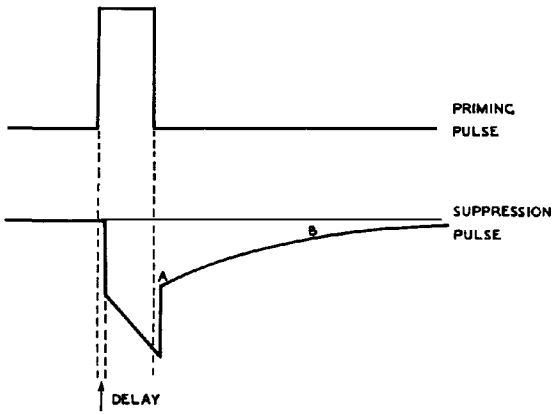

Fig.739 - Waveform of suppression pulse providing swept gain.

Of these the first is usually preset, the last two being under the control of the operator. When the controls are correctly adjusted all echoes from comparable objects are received at about the same amplitude, the appearance of the screen being roughly as in Fig.740. It will be noticed that as the gain increases along the time-base sweep the noise level rises also.

With a PPI display the setting of the temporal gain control differs from that needed with an A-type display since, even with equal echoes, the painting of the PPI is more intense nearer the centre. By the use of the controls the suppression waveform may be adjusted to give a reasonably uniform painting of targets, at all ranges.

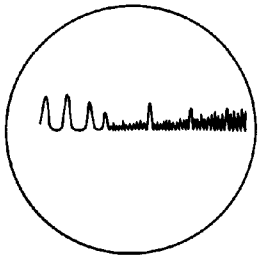

Fig.740 - A-type display with swept gain

This Page Intentionally Blank